Check for updates

Impact of Boundary Layer Physics on Tropical Cyclone Simulations in the Bay of Bengal Using the WRF Model

J. R. Rajeswari,[1,2] C. V. Srinivas,[1,2] P. Reshmi Mohan,[1,2] and B. Venkatraman[1,2]

Abstract—In this work, the sensitivity of tropical cyclone (TC) simulations over the Bay of Bengal to planetary boundary layer (PBL) physics in the WRF model is investigated. Numerical simulations are performed with WRF-ARW model using NCEP GFS data for five very severe cyclonic storms (Vardha, Hudhud, Phailin, Lehar and Thane). Five conceptually different PBL schemes (YSU, MYJ, QNSE, MYNN and BouLac) are evaluated. Results of 25 sensitivity experiments showed that PBL physics mainly affected the intensity while producing small variations in track prediction. The QNSE, followed by MYJ and BouLac, produced highly intensified storms, and MYNN produced weakly intensified storms. The YSU scheme showed better comparisons with IMD best track estimates. From the analysis of five cyclones, it is found that the YSU produced minimum errors for central pressure (-5.4, -0.8, -2.6, -5.25 hPa), maximum wind (19, 7.6, -0.96, -0.77 m/s) and track (66, 146, 182, 217 km) at 24-, 48-, 72- and 96-h forecast intervals. Analysis of various thermodynamical and dynamical parameters clearly showed that the PBL physics impacts the predictions by variation of (1) surface energy fluxes, (2) convergence, (3) inflow/outflow, (4) tangential winds, (5) vertical motion and (6) strength of the warm core and associated storm structure. A detailed analysis conducted in the case of Hudhud indicated that the PBL schemes influenced the intensity predictions through a WISHE type of feedback by the variation of convergence, radial inflow, vertical motion, and surface fluxes. While the YSU and MYNN schemes produced moderate values of radial inflow, the QNSE, MYJ and BouLac schemes produced stronger inflow. The stronger inflow, spin-up and stronger wind-induced transport of energy fluxes in the QNSE, MYJ and BouLac schemes led to a stronger convection and a higher intensification of TCs in these simulations.

Keywords: Tropical cyclone, WRF, simulation, PBL physics, intensity.

[1] Health, Safety and Environment Group, Indira Gandhi Centre for Atomic Research, Kalpakkam, Tamilnadu 603102, India. E-mail: cvsri@igcar.gov.in; venkatasrinivasc@yahoo.com
[2] Homi Bhabha National Institute, Anushakti Nagar, Mumbai 400094, India.

1. Introduction

Tropical cyclones (TC) are one of the most disastrous weather phenomena that form over warm tropical oceans. TCs are rotational wind systems in the tropics characterized by a large central pressure deficit and strong winds. They cause enormous damage to life and infrastructure during their landfall along the coastal areas due to heavy winds, storm surge and rainfall. TCs in the North Indian Ocean (NIO) are quite variable in their movement and intensity (Raghavan and Sen Sarma 2000). Though cyclones are largely steered by large-scale flows and the Coriolis force (Gray 1968), the actual movement is a result of complex interactions between the cyclone's internal and external influences. Accurate forecasting of TCs is critical for early warning and disaster management, and it is a challenging task for meteorological agencies. Over the past few decades, numerical models have shown considerable progress in TC track prediction due to increased model resolution, improved physics and quality initial conditions (Houze et al. 2007; Miyoshi et al. 2010; Rogers et al. 2006; Rappaport et al. 2009). However, intensity prediction is still lacking skill (Braun and Tao 2000) as it involves complex physical and dynamical processes in the inner core and its modulation by the large-scale environment.

The chief source of energy for the development of TCs comes from the ocean surface in the form of heat and moisture fluxes (Byers 1944; Emanuel 1986). The transfer of energy at the air–sea interface and within the atmosphere is controlled by the planetary boundary layer (PBL) characteristics. The PBL characteristics play a crucial role in the development of TCs. The vertical turbulent mixing in the PBL can

influence the air–sea exchange of moisture, heat and other physical parameters (Garratt 1994; Stull 1988). In addition, the friction in this region gives the initial spin-up for the development of the system. The PBL processes also facilitate the air–sea interaction with the moist conditionally symmetrical neutral upward flow through the secondary circulation in the eye wall (Emanuel 1986). The evolution of the thermodynamical and kinetic properties of the TC depends on the exchange of energy and momentum by sub-grid-scale eddies at the ocean surface. The explicit inclusion of sub-grid-scale eddies in the mesoscale model is not possible. So their effects are expressed through parameterization schemes (Stull 1988; Holton 2004; Stensrud 2007). The PBL is a vital part of TCs, as the energy transfer from the ocean surface to the atmosphere occurs through the PBL, and friction within the PBL modulates the low-level flow convergence. The strength of the winds in this region determines the flow convergence as well as the degree of energy transfer and thus ultimately the amount of convection and intensity of the storm. The boundary layer friction plays a dual role in tropical cyclones. It leads to the frictional convergence of the flow in the moist surface layer and also for the transfer of the latent heat to the system (Ooyama 1969). The PBL influences the intensification of the tropical cyclone by the radial convergence of momentum within the boundary layer (Smith and Thomsen 2010). As the spin-up of the vortex is associated with the dynamics of the boundary layer, the representation of PBL physics in numerical models is important in predicting TC intensification.

Recent modeling studies show large biases in TC intensity and track predictions due to uncertainties in the initial conditions and sensitivity to physics parameterizations (Parker et al. 2017; Khain et al. 2016; Ma and Tan 2009; Miglietta et al. 2015). Studies using both numerical modeling (Braun and Tao 2000; Hill and Lackmann 2009; Nolan et al. 2009a, b; Smith and Thomsen 2010; Kepert 2012; Kanada et al. 2012; Banks et al. 2016; Kumari et al. 2019; Loh et al. 2011) and observational analysis (Powell 1982; McBride and Zehr 1981; Franklin et al. 2003; Kepert 2006a, b) have examined the influence of PBL parameterization on TCs. Earlier studies (Kanada et al. 2012; Davis et al. 2008; Wada and

Usui 2010; Braun and Tao 2000; Gopalakrishnan et al. 2013; Montgomery et al. 2010; Nolan et al. 2009a, b; Smith and Thomsen 2010; Srinivas et al. 2007, 2013) suggest that the PBL can alter the primary and secondary circulation, which in turn affects the track changes, intensity, structure and precipitation. Direct measurements of TCs are available from only a few experiments, such as the Coupled Boundary Layer Air Sea Transfer (CBLAST) experiments (Black et al. 2007; French et al. 2007; Drennan et al. 2007; Zhang et al. 2008). Braun and Tao (2000) carried out high-resolution simulations of hurricane Bob using the MM5 model with four PBL parameterizations. The sensitivity tests indicated significant differences in the predicted cyclone intensity, with maximum winds varying up to 15 ms^{-1}. Their results based on detailed observation comparisons indicated significant differences; in particular, the MYJ scheme produced larger frictional tendencies, leading to stronger lower tropospheric inflow and a stronger azimuthal wind maximum at the top of the PBL, than the YSU scheme. Studies by Hill and Lackmann (2009) and Nolan et al. (2009a, b) on Atlantic hurricanes using different versions of WRF have shown that the higher-order Mellor–Yamada–Janjic turbulence kinetic energy (TKE) scheme produces considerably higher intensity estimates than the simple first-order non-local YSU scheme. Recent studies of Atlantic hurricanes using the high-resolution (3 km) HWRF model (Gopalakrishnan et al. 2011) suggest that PBL vertical diffusion has a strong influence on TC intensity by strengthening inflow, increasing the spin of the storm and enhancing the equivalent potential temperature in the PBL, thereby leading to a stronger and warmer core. In recent times, high-resolution numerical models have been increasingly used, as they resolve the topography and surface dynamical and thermodynamical processes which consequently influence the evolution of the PBL and weather processes (Zhang and Anthes 1982; Rajeswari et al. 2020; Milovac et al. 2016). Li and Pu (2009) conducted numerical experiments to analyze the sensitivity of the early rapid intensification of TC Emily (2005) at different horizontal resolutions. Their study showed that at 3-km grid spacing, the PBL processes had a significant impact on the storm

convective and precipitation structures and corresponding storm intensity.

The Weather Research and Forecasting (WRF) model has been used for operational weather forecasting and emergency preparedness programs in the Indian Ocean region (Roy Bhowmik 2013; Raja Shekhar et al. 2020). There are several studies on the prediction of TCs over the NIO region in terms of physics sensitivity and data assimilation (Bhaskar Rao and Hari Prasad 2007; Mukhopadhyay et al. 2011; Krishna et al. 2012; Srinivas et al. 2007, 2013; Saikumar and Ramashri 2017; Raju et al. 2011; Chandrasekar and Balaji 2012; Rambabu et al. 2013; Rai and Pattnaik 2018; Greeshma et al. 2019; Malakar et al. 2020; Mohanty et al. 2019; Mohan et al. 2019 among others). Srinivas et al. (2013) studied the impact of WRF physics with 65 sensitivity experiments for five severe TCs at 9-km resolution during the period 2000–2011 and found that the non-local YSU scheme gave more realistic prediction of winds in the inflow region and intensity and track predictions compared to the 1.5 order MYJ local TKE-based diffusion scheme and non-local first-order ACM scheme. Singh and Bhaskaran (2017) studied the performance of WRF for TCs in the Bay of Bengal (BOB) during 2013. It was suggested that the non-local YSU along with the simplified Arakawa-Schubert (SAS4) convective parameterization produced the best predictions for intensity and track estimates. Kumari et al. (2019) studied the sensitivity of WRF simulations of seven TCs in the BOB to the model PBL schemes using 9-km resolution. It was suggested that local and non-local PBL schemes produce different impacts on the intensity and track forecasts depending on the intensity stage of the TC at which the model is initialized. Rai and Pattnaik (2018) conducted a numerical analysis of structure and intensity of TC Phailin with five PBL parameterizations and observed that during the pre-intensification phase of the TC, the track and intensity are not very sensitive to PBL parameterization, but structural changes were observed. It has been shown that a significant sensitivity of track and intensity to PBL parameterizations is observed during a rapid intensification phase. The WRF model has been upgraded with several advanced physics schemes, and it is necessary to test the model performance

using sensitivity tests for better predictions. The preceding review shows that compared to the large number of sensitivity studies on Atlantic hurricanes, relatively few studies exist for TCs in the NIO focusing on the influence of PBL physics. Most of the physics sensitivity studies for TCs over the NIO are confined to a few cyclone cases at grid sizes of ≥ 9 km using only a few PBL schemes and with limited insights, not leading to clear inferences on their application to operational predictions.

With this gap, the present study aims to examine the performance of the WRF model with different PBL physics on the intensity and track predictions for tropical cyclones over the BOB of the NIO at 3-km horizontal resolution. Five cyclones formed in the BOB during 2011–2016 were considered for the study. The objectives of the present study are to (1) examine the sensitivity of structure and internal dynamics that contribute to changes in the intensity of TCs to different types of PBL physics and (2) compare high-resolution simulations in the present work with the earlier results using 9-km resolution (Srinivas et al. 2013) for differences. Section 2 gives a description of the cyclones selected in the study, and Sect. 3 gives a brief description of the model and the PBL physics schemes used for the simulations. Section 4 provides detailed results of various simulated parameters, and Sect. 5 gives the salient conclusions of the study.

2. Tropical Cyclone Cases

In this study, five tropical cyclones (Thane, Lehar, Phailin, Hudhud and Vardha) which formed over the BOB during the period 2011–2016 are chosen for simulations to assess the sensitivity of PBL physics in the WRF model. Among the five cases, Thane and Vardha originated in the southeastern BOB, Phailin and Hudhud formed over the eastern central BOB and Lehar over the Andaman Sea from a remnant cyclonic circulation over the South China Sea. A description of these cyclones is given in the bulletins of the Regional Specialized Meteorological Centre (RSMC) for Tropical Cyclones, New Delhi (India Meteorological Department, 2010–2017). Details regarding the duration, intensity category, landfall

Table 1

Details of the selected tropical cyclones in the study

Cyclone (year)	Duration	Category (MSW in m/s and min CSLP in hPa)	Landfall position	Model simulation period (YYYYMMDDHH)
Vardha (2016)	8–13 December	VSCS (70, 975)	Chennai, TN	2016120800–2016121300
Hudhud (2014)	8–13 October	ESCS (100, 950)	Visakhapatnam, AP	2014100800–2014101300
Phailin (2013)	9–13 October	ESCS (115, 940)	Gopalpur, Odisha	2013100900–2013101300
Lehar (2013)	24–28 November	VSCS (75, 980)	Machilipatanam, AP	2013112400–2013112809
Thane (2011)	26–30 December	VSCS (75, 969)	Cuddalor, TN	2011122700–2011123006

VSCS very severe cyclonic storm, *ESCS* extremely severe cyclonic storm, *TN* Tamil Nadu, *AP* Andhra Pradesh, *MSW* maximum surface winds, *CSLP* central sea level pressure

positions and the simulation period of the five TC cases selected for the study are given in Table 1. The IMD best tracks of all five TC cases are given in Fig. 1b.

3. Model Configuration

The Advanced Research Weather Research and Forecasting (WRF-ARW) model version 3.8 is used for the simulations. It is a 3D non-hydrostatic primitive equation mesoscale model (Skamarock et al. 2008) developed by the National Centre for Atmospheric Research (NCAR). The model uses a terrain-following hydrostatic pressure vertical coordinate and an Arakawa C-type horizontal grid. This model has several options for spatial discretization, diffusion, nesting, lateral boundary conditions, data assimilation and physics. In the present study, the WRF-ARW model is configured with three interactive nested
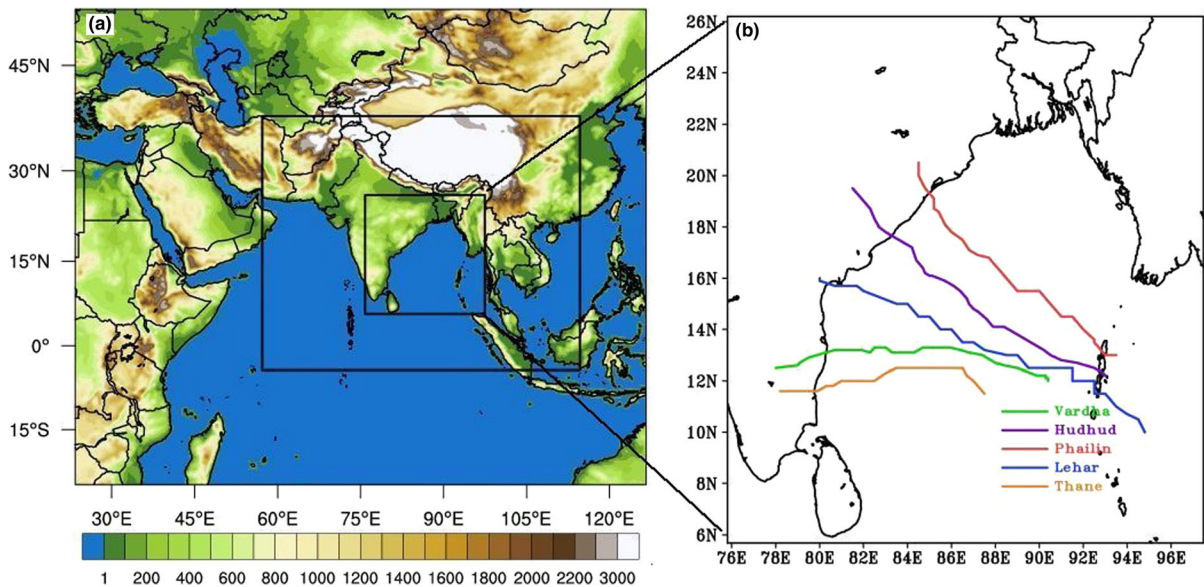

Figure 1
a Simulation domains used in the WRF model and **b** the actual tracks of all five selected TC cases in the BOB according to IMD

domains with horizontal resolutions of 27 km, 9 km and 3 km, respectively (Fig. 1a). The simulation for each cyclone is initialized at a deep depression stage as given in Table 1. The India Meteorological Department (IMD) defines (http://www.imdpune.gov.in/Weather/Reports/glossary.pdf) a deep depression as an intense low-pressure system represented on a synoptic chart by two or three closed isobars at a 2-hPa interval and wind speed from 28 to 33 knots at sea level and three to four closed isobars in the radius of 3 degrees from the center over land. The initial conditions are specified from the National Center for Environmental Prediction (NCEP) Global Forecasting System (GFS) $0.25° \times 0.25°$ analysis, and the boundary conditions are updated every 3 h. Except for the PBL, the other physics options are chosen based on earlier studies conducted for the TCs over the Bay of Bengal (Srinivas et al. 2013; Raju et al 2011, 2012). The physics options included in the model are the Kain–Fritsch scheme (Kain 2004) for cumulus parameterization, the 6-hydrometeor class Thompson scheme for cloud microphysics (Thompson et al. 2008), the Noah scheme (Chen and Dudhia 2001) for land surface processes, and the RRTMG scheme (Iacono et al. 2008) and the Dudhia scheme (Dudhia 1989) for long-wave and short-wave radiation transfer, respectively. The KF scheme is used only in the outer domains with 27-km and 9-km resolutions. In the fine-resolution 3rd domain, only the Thompson microphysics scheme is used for convection. Five numerical simulations with different PBL parameterization schemes are conducted for each cyclone cases, keeping all the other physics options fixed.

Five PBL physics schemes (YSU, MYJ, QNSE, MYNN and BouLac) are used in the present study. In the WRF-ARW model, the PBL parameterization schemes can be classified into two categories; local and non-local schemes (Stensrud 2007). According to local closure, the unknown quantity at any point in space is parameterized by values and/or gradients of known quantities at the same point in a local closure, and in the non-local schemes, it is parameterized by values of known quantities at many points in space (Stull 1988; Hariprasad et al. 2014; Banks et al. 2016; Srinivas et al. 2018) . The Yonsei University (YSU) scheme is a first-order non-local scheme (Hong et al.

2006) with a parabolic K-profile in an unstable mixed layer. It includes a term for counter-gradient flux for mixing by large eddies and an entrainment term for mixing of stable air with the unstable air within the PBL. The PBL height is calculated using the critical Richardson number. The Mellor–Yamada–Janjic (MYJ) scheme (Janjic 1994; Mellor and Yamada 1974, 1982) is a 1.5-order scheme using local vertical mixing, where the vertical diffusion is formulated through TKE. The Mellor–Yamada–Nakanishi–Niino (MYNN) level 3 scheme (Nakanishi and Niino 2006) is a second-order scheme based on TKE with a local vertical mixing. In order to improve the insufficient growth of the convective boundary layer and underestimation of TKE in the Mellor–Yamada schemes (1974, 1982), the MYNN scheme is tuned with large eddy simulations (LES). The quasi-normal scale elimination (QNSE) scheme (Sukoriansky et al. 2005) is a 1.5-order local closure and the prognostic equation of TKE which uses new theory for a stably stratified region to account for the wave phenomena within the stable boundary layer. In the QNSE scheme, mixing in the unstable and neutral situations is calculated using the MYJ 1.5-order closure formulation (as in the MYJ scheme), and for stably stratified conditions, the original QNSE model is used. To account for the transport processes on the eliminated scales in the QNSE scheme, ensemble averaging over infinitesimally thin spectral shells yielding scale-dependent horizontal and vertical eddy viscosities and eddy diffusivities are used. Through this, it could include the waves and turbulent anisotropy. The Bougeault–Lacarrere (BouLac) scheme (Bougeault and Lacarrere 1989) is a 1.5-order local scheme with a prognostic equation for TKE. The TKE of the BouLac scheme has the same formulation as in MYNN2, but the eddy diffusivity differs in terms of formulation of the stability function and length scale. The formulation of the stability function indicates that the BouLac scheme favors a highly unstable condition in the PBL. The surface energy fluxes are calculated using the MM5 surface layer scheme in the case of YSU, MYNN and BouLac schemes, and the Eta similarity scheme in MYJ and QNSE schemes.

4. Results and Discussion

The Results and Discussion section is divided into two parts. The first part deals with the track and intensity analysis of all the selected five cyclone cases, and the second part consists of a more detailed structural and intensity analysis of cyclone Hudhud. The first 12 h of the simulation is considered as the spin-up period of the model, and simulation results are compared with observational estimates eliminating the spin-up time.

4.1. Track Predictions

The simulated tracks of all the five cyclones are analyzed and compared with the IMD best track data (Fig. 2). The track errors with the five PBL schemes increased from initial to final stages during the life cycle of the TC in all the simulations. However, the track errors are nearly similar till 36–48 h, but varied widely thereafter. Srinivas et al. (2013) also have found similar results for cyclone Sidr with three PBL schemes. This suggests that PBL schemes have very little influence on track predictions during the initial stages of cyclones. It is noted that YSU and MYNN schemes produced comparatively better results than the other schemes throughout the life cycle for most of the cyclones simulated. Simulated tracks for Vardha, Phailin and Thane are closely dispersed, and those for Hudhud and Lehar are widely dispersed. Simulated tracks are aligned to the north of the observed track for cyclones Vardha and Thane and to the southwest for cyclone Phailin. The simulated tracks of cyclones Hudhud and Lehar are aligned on either side of the observed tracks. Simulated tracks followed a west-northwesterly direction for cyclones Vardha and Thane and north-westerly direction for cyclones Hudhud, Phailin and Lehar. The strong easterly large-scale winds (16 knots) steered Vardha and Thane to the west and show minimum deviations in simulations with different PBL physics. Hudhud and Phailin formed in October which is the transition period from the southwest monsoon to the northeast monsoon with a weaker synoptic wind system. With the onset of the NE monsoon, the strong NE winds restrict the northward propagation of TCs. Wide dispersion is found in the simulated tracks for cyclones Hudhud and Lehar (Fig. 2b, d) which moved to the northwest. Figure 3 shows the time variation of track errors with respect to the IMD estimates for experiments with different PBL physics for each cyclone. The mean track errors for all PBL physics are 31, 208, 278 and 330 km for Vardha, 62, 57, 62 and 150 km for Hudhud, 62, 165, 146 and 312 km for Phailin, 108, 151, 233 and 158 km for Lehar, and 91, 168, 223 and 0 km for Thane at 24, 48, 72 and 96 h, respectively. In the case of Thane, all the schemes produced a similar order of track error at different forecast intervals. The large deviation in the track from the observation by all the schemes is apparently due to the fact that the simulation of the tropical cyclone movement is not related to the PBL schemes but due to issues related to model dynamics and initialization. The minimum track errors are produced by YSU and BouLac for Vardha, YSU and MYNN for Hudhud, QNSE, YSU and BouLac for Phailin, MYNN and YSU for Lehar, and MYNN and QNSE for Thane. Overall, for all five cyclones, YSU followed by MYNN produced the lowest track errors (66, 146, 182 and 217 km at 24, 48, 72 and 96 h, respectively), while QNSE followed by MYJ and BouLac produced the largest track errors (63, 163, 197 and 242 km at 24, 48, 72 and 96 h, respectively) (Table 2, Fig. 6). The results of this study with YSU and MYJ producing the lowest and highest track errors, respectively, confirm the earlier findings by Srinivas et al. (2013) for Sidr. The present results gain further significance due to application for a relatively large number of samples (five cyclones in the NIO region for the sensitivity experiments) and at high resolution (3 km). Though both MYNN and MYJ are based on TKE closure, MYJ produced larger errors compared to MYNN. The track differences in the two cases could be due to variation in the turbulent length scale and eddy diffusivity in MYNN which considers effects of stability (Nakanishi and Niino 2009). The MYNN scheme produced nearly similar results to the first-order non-local YSU scheme, while results of MYJ are closer to QNSE. The track errors among different simulations varied by 5–20% at 24–96-h forecast intervals, indicating only a small impact by PBL physics. This indicates that the PBL physics influences the track predictions mainly during the

peak growth and decay phases, as also found by Rai and Pattnaik (2018). The variation in tracks among simulations with different PBL physics could be due to changes in the thermodynamics and dynamics induced by the differential transport of momentum and moisture, which are analyzed in the subsequent sections. Overall, we observe small variations in the track predictions with different PBL schemes (Fig. 6). The poor prediction skill of the WRF model for westward-moving cyclones was also reported in Srinivas et al. (2013), and the same is observed for Vardha and Thane in the present study. The differences between simulation results and IMD estimates could be due to the error in the IMD best track data for cyclones in the NIO region. This data is derived using all available surface and upper-air observations from land and ocean, satellite observations and radar observations and following the Dvorak technique (IMD 2003). Owing to limited observations in the NIO, the best track estimates are prone to errors as they are mostly estimated with the satellite imagery interpretation by Dvorak's technique. The mean error in best track may be taken as 50 km (http://www.rsmcnewdelhi.imd.gov.in/images/pdf/archive/best-track/bestrack.pdf).

4.2. Intensity Predictions

The intensity of each cyclone is examined based on the central sea level pressure (CSLP) and maximum sustained wind (MSW) speed. The time series of simulated CSLP of the five cyclones (Vardha, Hudhud, Phailin, Lehar and Thane) for different PBL schemes is compared with the IMD best track data (Fig. 4). Generally, it is observed that for a majority of the cyclones, all the simulations overestimated the pressure drop as compared to the IMD estimates, except for Thane where all the schemes underestimated the pressure drop. In general, except for Thane, all the PBL schemes show higher pressure drop compared to the IMD estimates. All the simulations for Vardha show a rapid deepening indicating early attainment of peak intensification about 24 h before the actual. For Hudhud, MYNN and YSU produced better simulation of CSLP than the other schemes. QNSE, BouLac and MYJ show early intensification by 12 h. For Lehar, all the simulations show gradual

deepening up to 60 h, in good agreement with IMD data, but subsequent to 60 h, a sudden and large pressure fall is observed, indicating attainment of peak intensification about 12 h after the actual. For Lehar, YSU, QNSE and BouLac produced better simulation of CSLP before the peak intensification, and MYJ and MYNN during the peak growth and decay, than the other schemes. For Hudhud and Phailin, all the simulations followed the observed trends in CSLP evolution, but MYNN and YSU produced better comparison with IMD estimates. All the other schemes produced different results for different cyclone cases. It is observed that the maximum deviation in CSLP for all the cyclones is produced by the QNSE scheme followed by the BouLac scheme. For Vardha, the maximum pressure deficit produced is 25 hPa with QNSE and BouLac and 15 hPa with MYNN against the actual pressure deficit of 20 hPa. The maximum pressure deficit produced for Hudhud is 65 hPa with QNSE and 35 hPa with MYNN against the actual 35 hPa. For Phailin, the simulated maximum pressure deficit is 60 hPa with QNSE and 40 hPa with MYNN against the actual 40 hPa. The simulated maximum pressure deficit for Lehar is 55 hPa with QNSE and 25 hPa with MYNN against the actual pressure drop of 20 hPa. The maximum pressure deficit produced for Thane is 20 hPa with QNSE and 10 hPa with MYJ against the actual pressure deficit of 30 hPa. For Thane, none of the simulations could represent the intensification of the cyclone. This suggests the need for further investigations focusing on the dynamics and initialization to understand the model's lack of success in simulating TC Thane. Overall, for all five cyclones, the YSU scheme produced the lowest CSLP errors (-5.4, -0.8, -2.6, -10.0, -5.25 hPa) and QNSE produced the highest errors (-5.0, -8.0, -11.2, -24.0, -11.8 hPa) at 24, 48, 72, 84 and 96 h, respectively.

The time evolution of MSW of the five cyclones with the five PBL schemes are compared with IMD estimates (Fig. 5). A fall in pressure is followed by an increase in wind speed during the growing and peak phases. The winds are overestimated for Vardha, Hudhud and Lehar, indicating stronger simulated cyclones, and are underestimated for Phailin and Thane, indicating weaker simulated cyclones in these
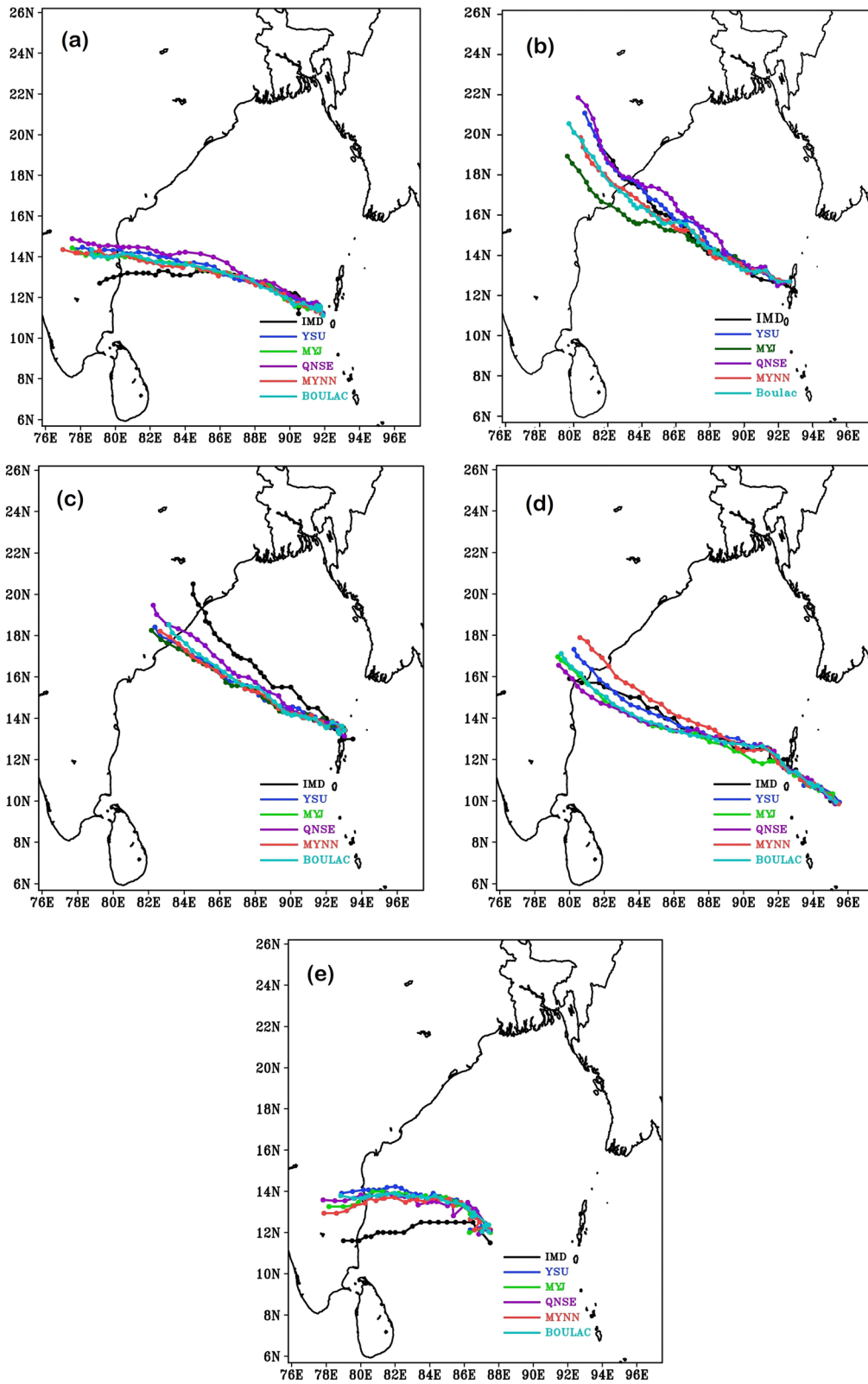
◀Figure 2
Simulated vector tracks of the five selected TCs along with the IMD observational track for **a** Vardha, **b** Hudhud, **c** Phailin, **d** Lehar, **e** Thane

cases. Like CSLP, the evolution of winds shows an early intensification for Vardha and a late intensification for Lehar in simulations. For most of the cyclones, the MSW is overestimated by QNSE, BouLac and MYJ, better simulated by YSU and underestimated by MYNN compared to the IMD estimates. For Vardha and Hudhud cyclones, the YSU followed by MYNN produced winds in good agreement with the IMD estimates, while QNSE, BouLac and MYJ slightly overestimated the winds. For Phailin and Thane cyclones, the QNSE followed by BouLac, YSU and MYJ schemes produced winds in better agreement with IMD estimates, while MYNN considerably underestimated the winds during the period of maximum intensification. For Lehar, while all the schemes overestimated the winds from 72 h to 96 h, during the growing stages, MYNN considerably underestimated the winds, QNSE and BouLac overestimated the winds and MYJ and YSU produced close estimates.

Figure 6 shows the mean percentage error in MSW and CSLP calculated with respect to IMD estimates at 12-h intervals produced by each PBL scheme for all five cyclones. A positive value indicates an overestimation by the model and vice-versa. In general, while MYNN underestimated the winds by ∼ 5 to 12% throughout the life cycle, all the other schemes overestimated the winds to different degrees (YSU: −2 to 25%; MYJ: 5–22%; BouLac: 8–28%; QNSE: 15–30%). During the period of maximum intensification (48–84 h), the YSU scheme produced the minimum error (+ 3%), followed by MYJ (+ 6%) and MYNN (−10%), while the BouLac and QNSE schemes produced the maximum error of +22% which indicates a high degree of overprediction. All the schemes produced gradually decreasing errors in the growing phase, minimum errors during peak intensification followed by increase in error toward the decaying phase. These results suggest that the YSU followed by MYJ

schemes produced comparatively small MSW errors during the growing and peak intensification period. The mean MSW errors for all five cyclones are lowest with YSU (19, 7.6, −0.96, −0.77 m/s) and highest with QNSE (28.5, 16.8, 13.4, 7.0 m/s) at 24, 48, 72 and 96 h, respectively.

Figure 6b shows the mean percentage error produced in CSLP simulation by all five schemes calculated for the five TCs at an interval of 12 h. The negative CSLP errors associated with the PBL schemes at most of the time steps indicate underestimation of central pressure and thus an overestimation of intensity. The CSLP errors indicate the QNSE followed by BouLac and MYJ produced highly intensified storms. The maximum CSLP errors produced during the peak intensification period are −2.6, −1.2, −1.0, 0.8 and −0.5% for QNSE, BouLac, MYJ, YSU and MYNN, respectively, and they correspond well with the positive MSW errors (Fig. 6a). Overall, considering the variation in both MSW and CSLP, the YSU and MYJ schemes produced smaller errors and thus better simulated TC intensity. The variation in the turbulent length scale formulation between MYJ and MYNN affects the stability and buoyancy of the system, and this may lead to variation in the temperature and moisture distribution, warm core characteristics and radial and tangential winds. These are analyzed in the subsequent sections.

4.3. Structure of the Storm

Results in the previous sections clearly show that the QNSE, BouLac and MYJ produced stronger cyclones with larger track errors; YSU produced realistic results, while MYNN produced weaker cyclones. Both YSU and MYNN produced realistic track predictions. The differences in the simulations are analyzed from storm thermodynamics and wind flow characteristics such as warm core, vertical velocities, vorticity/divergence and radial and tangential wind distribution. Although this analysis was conducted for all the simulated cyclones, results are mainly illustrated for the TC Hudhud.
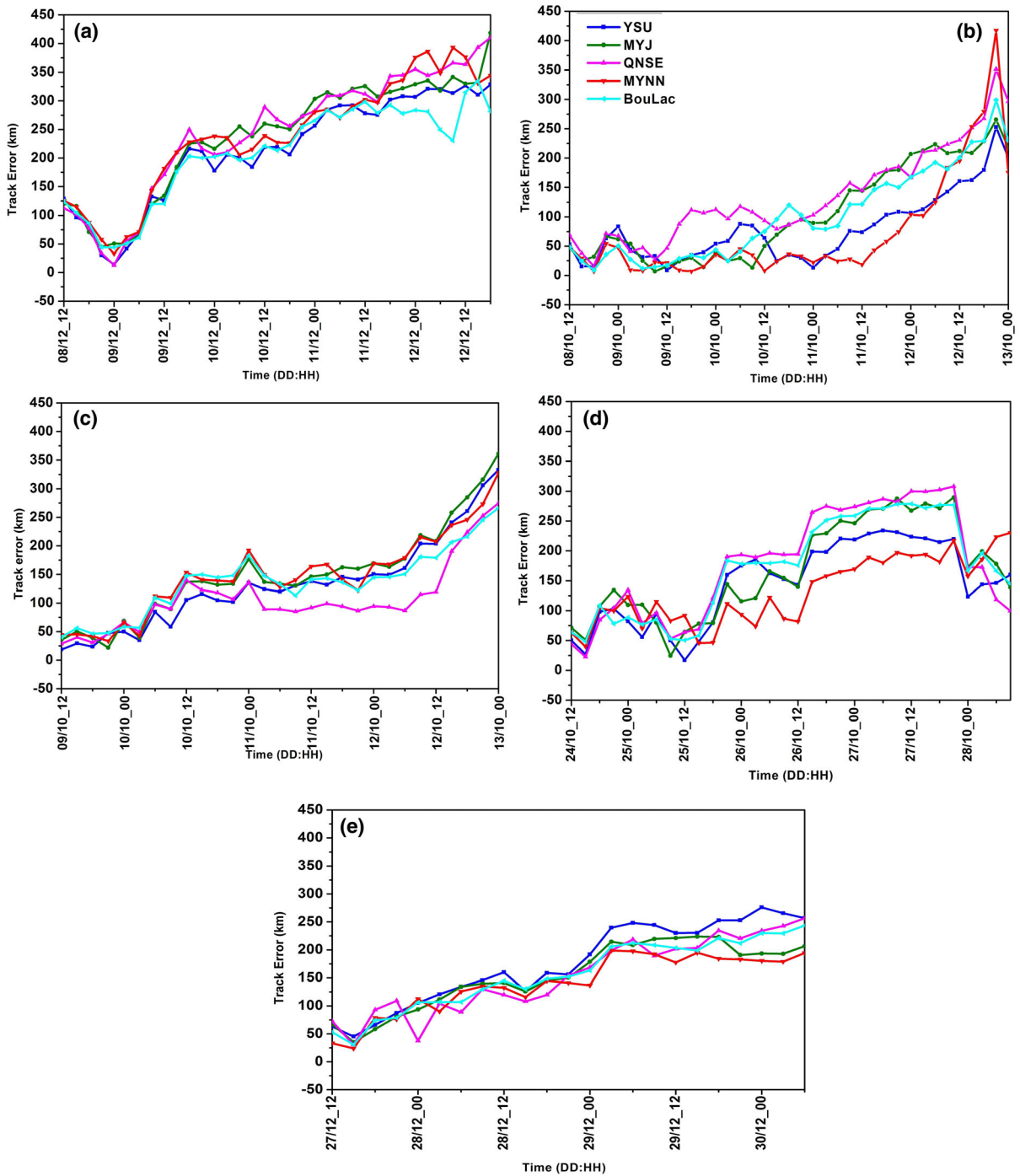
Figure 3
Time variation of vector track error with respect to the IMD best track estimates from simulations with different PBL physics for **a** Vardha, **b** Hudhud, **c** Phailin, **d** Lehar, **e** Thane

Table 2

Mean track, CSLP and MSW errors computed from 3-h interval model outputs for five tropical cyclones in the experiments with different PBL physics

Mean error in track (km)

Forecast interval (h)	YSU	MYJ	QNSE	MYNN	BouLac
24	66.9	76.9	63.7	76.3	69.6
36	83.3	98.5	108.2	116.0	96.1
48	146.8	145.2	163.3	139.2	154.0
60	158.7	163.5	174.2	134.0	163.2
72	182.9	200.4	197.6	164.3	195.8
84	194.7	236.4	218.9	179.9	219.5
96	217.4	267.4	242.2	241.1	221.0

Mean error in central sea level pressure (hPa)

Forecast interval (h)	YSU	MYJ	QNSE	MYNN	BouLac
24	−5.4	−2.2	−5	−2	−4.4
36	−4.8	−1	−5.8	1.6	−4.6
48	−0.8	4.2	−8	5.8	0.2
60	−1.2	3	−9	5	−3
72	−2.6	0	−11.2	5.6	−6.6
84	−10	−7.75	−24	−2	−15
96	−5.25	−4	−11.75	−1.5	−3.75

Mean error in maximum surface wind speed (m/s)

Forecast interval (h)	YSU	MYJ	QNSE	MYNN	BouLac
24	19.40	24.80	28.51	19.41	22.59
36	12.24	14.64	13.74	5.26	15.07
48	7.64	8.25	16.84	2.89	8.64
60	4.30	5.36	12.59	−5.1	4.99
72	−0.96	1.86	13.39	−6.30	4.20
84	1.17	3.76	11.55	−4.21	11.65
96	−0.77	0.71	7.04	−8.64	6.26

4.3.1 Radial and Tangential Wind Distribution

An important feature of the PBL related to TCs is the effective inward acting force that develops due to friction in the lower regions outside the eye wall (Nolan et al. 2009a). This inward force gives rise to strong inflow and spin-up of the inner core. Figure 7 shows the azimuthally averaged radial height cross section of radial winds in the lower atmosphere (up to 3 km) for cyclone Hudhud at its peak intensification stage (18 UTC 11 October 2014). The azimuthally averaged profiles provide the mean representation of distribution of the parameters. The negative wind indicates the inflow which is prominent below 2 km, and the positive winds which are prominent above the

2-km altitude indicate the outflow. The maximum radial wind speed is observed along the eye wall, and with moving toward the eye, the radial wind speed reduces to zero (Fig. 7). It is also clear that horizontal and vertical gradient exist for the radial wind distribution. The maximum inflow is observed at lower levels, and as the height increases, the intensity of inflow is reduced and outflow becomes prominent. In the lower regions (0–0.5 km), the QNSE simulated a stronger radial flow (31 m/s) over a wide area followed by the YSU and MYJ (26 m/s), BouLac (20 m/s) and MYNN (17 m/s). Similarly, in the middle and upper layers, the QNSE simulated a stronger outflow (8 m/s) followed by YSU (7 m/s), MYJ and MYNN (4 m/s) and BouLac (1 m/s). The stronger TC with QNSE may be related to the stronger upper-level outflow which leads to a decrease in surface pressure (Fig. 4b) and consequent increase in low-level inflow (Fig. 7c) near the inner core. The stronger inflow in the case of QNSE, YSU and MYJ leads to an increase of the angular momentum (spin) of the storm, potential temperature in the boundary layer, a stronger and warmer core and, thus, a stronger storm. The simulations with MYJ and MYNN show variation of about 9 m/s in the maximum radial wind. These differences may be attributed to the differences in the formulation of the turbulent length scale in MYJ and MYNN and to the higher surface exchange coefficient in the Eta surface layer associated with MYJ compared to the MM5 similarity surface layer scheme associated with the MYNN scheme. This variation leads to more energy transport from the ocean to the atmosphere for MYJ simulations and results in a stronger TC. The stronger turbulent diffusion in MYNN reduces the gradients between the surface layer and the PBL, thereby leading to a weaker frictional force and weaker inflow, as suggested by Gopalakrishnan et al. (2013).

Figure 8 shows the radius height cross section of an azimuthally averaged tangential wind profile for TC Hudhud at the time of its peak intensification (18 UTC 11 October 2014). The Cooperative Institute for Research in the Atmosphere (CIRA) multi-satellite analysis data was used for the comparison. The analyzed CIRA data is prepared from data collected by sensors of various satellites like SSM/I, AMSU, MODIS, QuikSCAT and ASCAT at horizontal
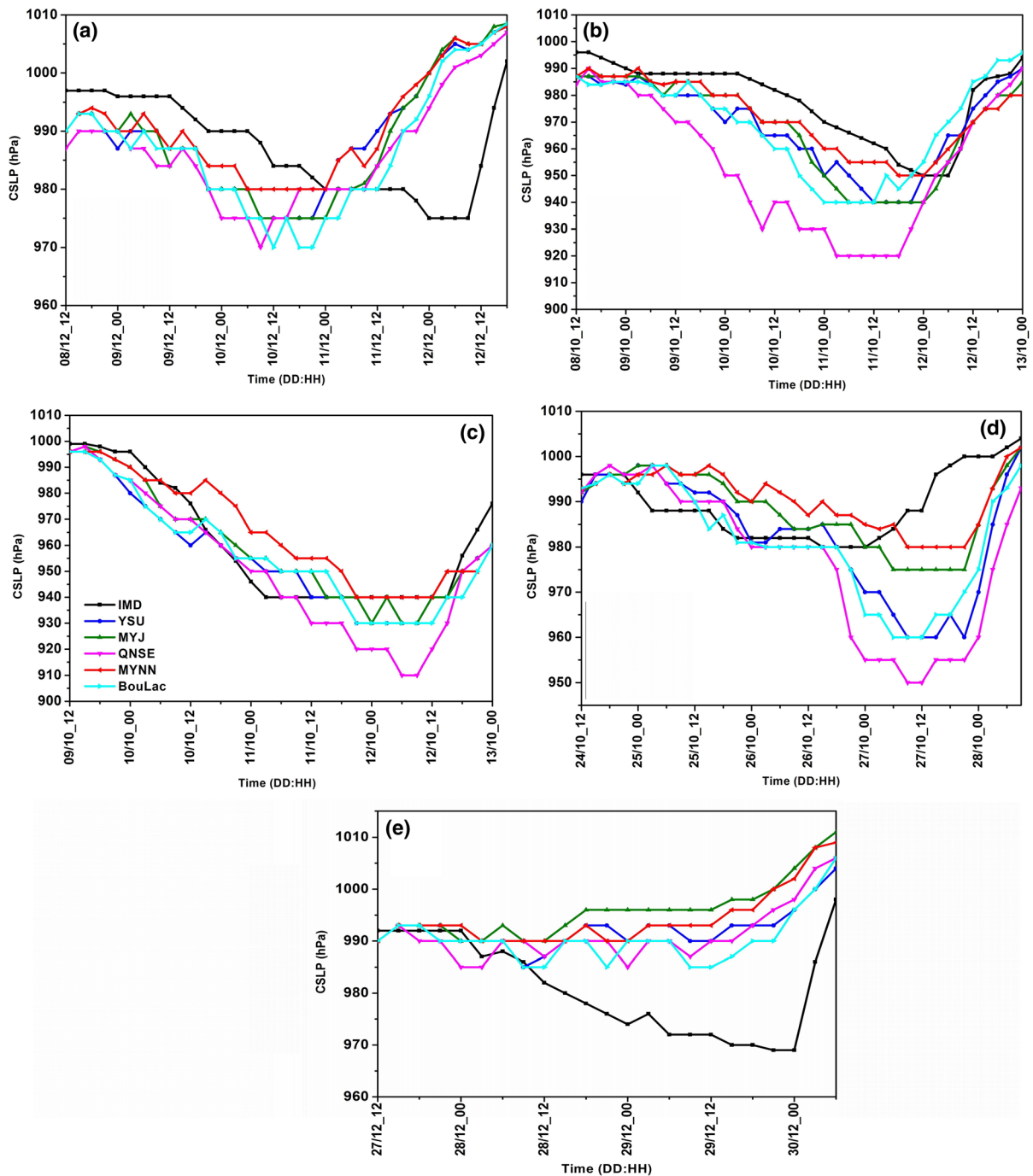
Figure 4
Time variation of central sea level pressure (hPa) from simulations with different PBL physics for **a** Vardha, **b** Hudhud, **c** Phailin, **d** Lehar and **e** Thane along with IMD observational data

resolutions of 25 km and above (Knaff et al. 2011). The model has a finer resolution (3 km) than the observation (25 km) and indicates stronger tangential winds than the coarse CIRA data. The profile of tangential wind in the CIRA data is observed as a smoothened one. The CIRA data (Fig. 8f) shows a
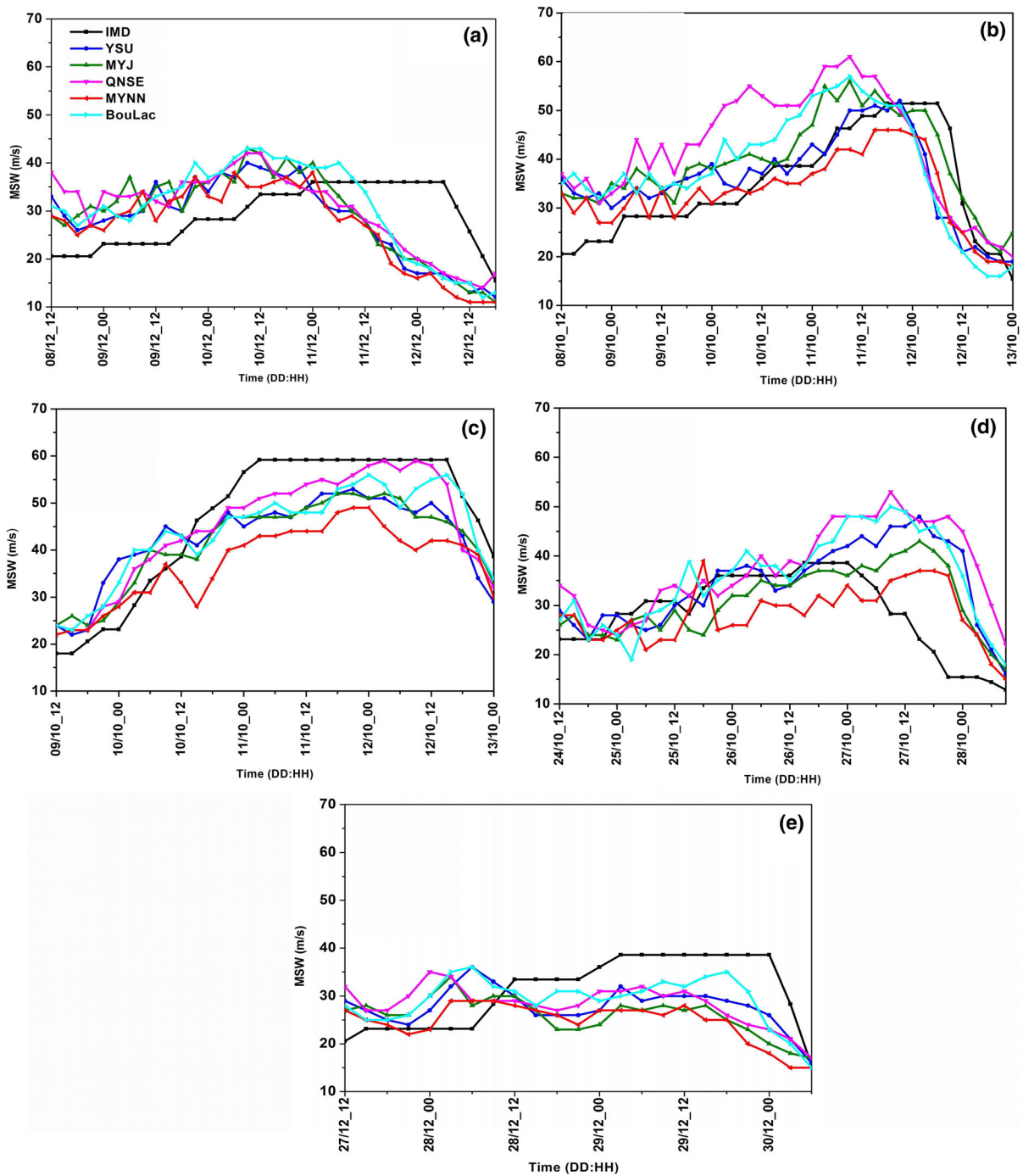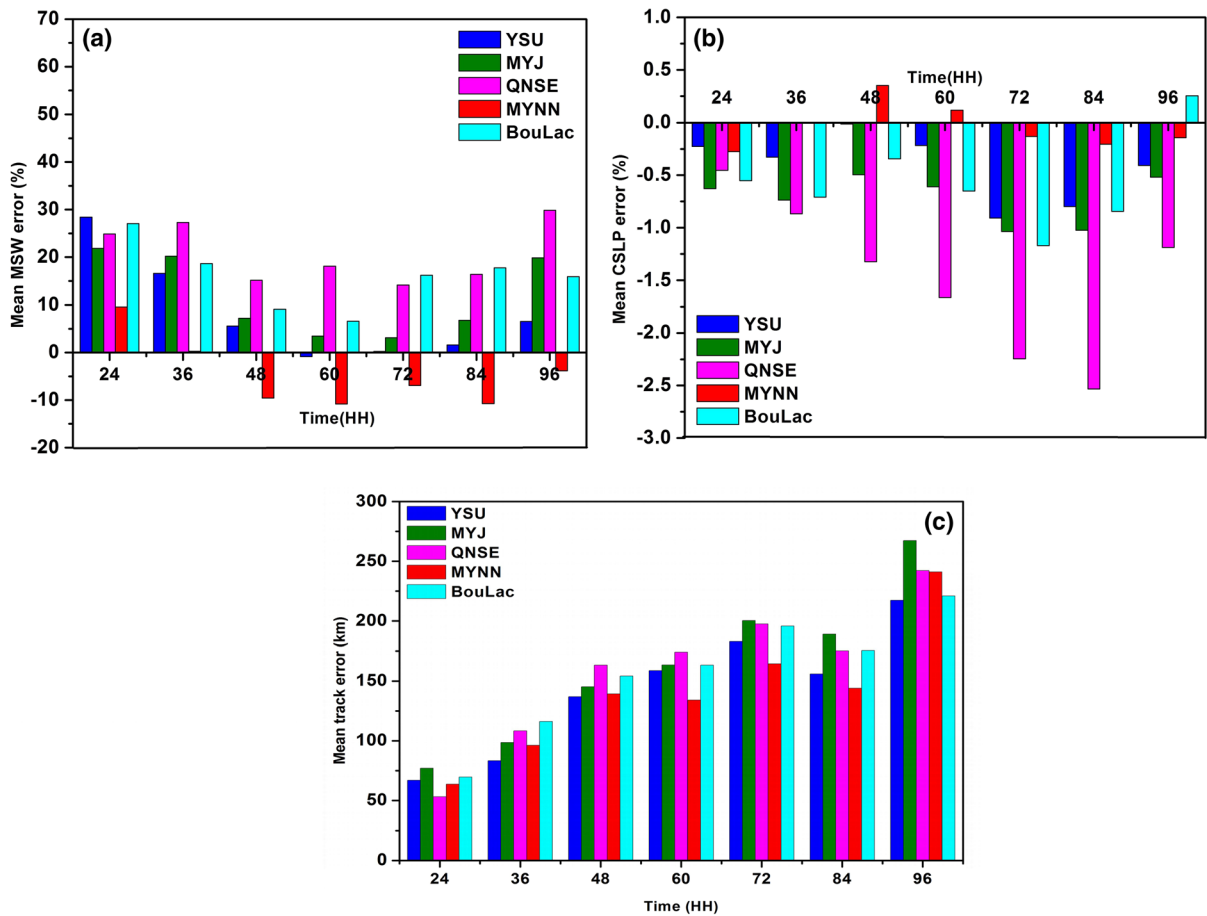
Figure 5
Time variation of maximum sustainable wind (m/s) from simulations with different PBL physics for **a** Vardha, **b** Hudhud, **c** Phailin, **d** Lehar and **e** Thane along with IMD observational data

Figure 6
Mean error in the simulated **a** MSW, **b** CSLP and **c** track with respect to IMD estimates for the selected five TCs from simulations with different PBL physics

maximum tangential wind speed of 50 m/s at a radius of about 100 km from the eye with vertical extent of 10 km, and the winds decrease both horizontally and vertically. The simulated maximum tangential wind speed is 80 m/s for the QNSE scheme, 65 m/s for the YSU and MYJ schemes, and 60 m/s for the MYNN and BouLac schemes. The stronger inflow in the boundary layer in QNSE, YSU and MYJ (Fig. 7) lead to stronger inward transport of angular momentum leading to more predominant tangential winds (Fig. 8) near the eye wall and consequent increase in TC intensity. The maximum winds are simulated at 80 km in MYNN and at 75 km in all the other simulations. The maximum winds extended vertically up to 8 km in YSU, 7 km in MYJ, 11 km in QNSE,

5 km in MYNN and 4 km in the BouLac scheme. The vertical extension of maximum winds is better simulated in QNSE and the horizontal extension in MYNN and YSU schemes. The azimuthal distribution clearly shows that the MYJ produces relatively stronger tangential winds compared to the MYNN scheme.

4.3.2 Storm Thermodynamics

To examine the energy transport from the ocean leading to the growth of the TC, the average sensible and latent heat energy fluxes over a $2° \times 2°$ area were computed along the track of the TC Hudhud (Fig. 9). The Modern-Era Retrospective Analysis for Research and Applications 2 (MERRA-2) reanalysis
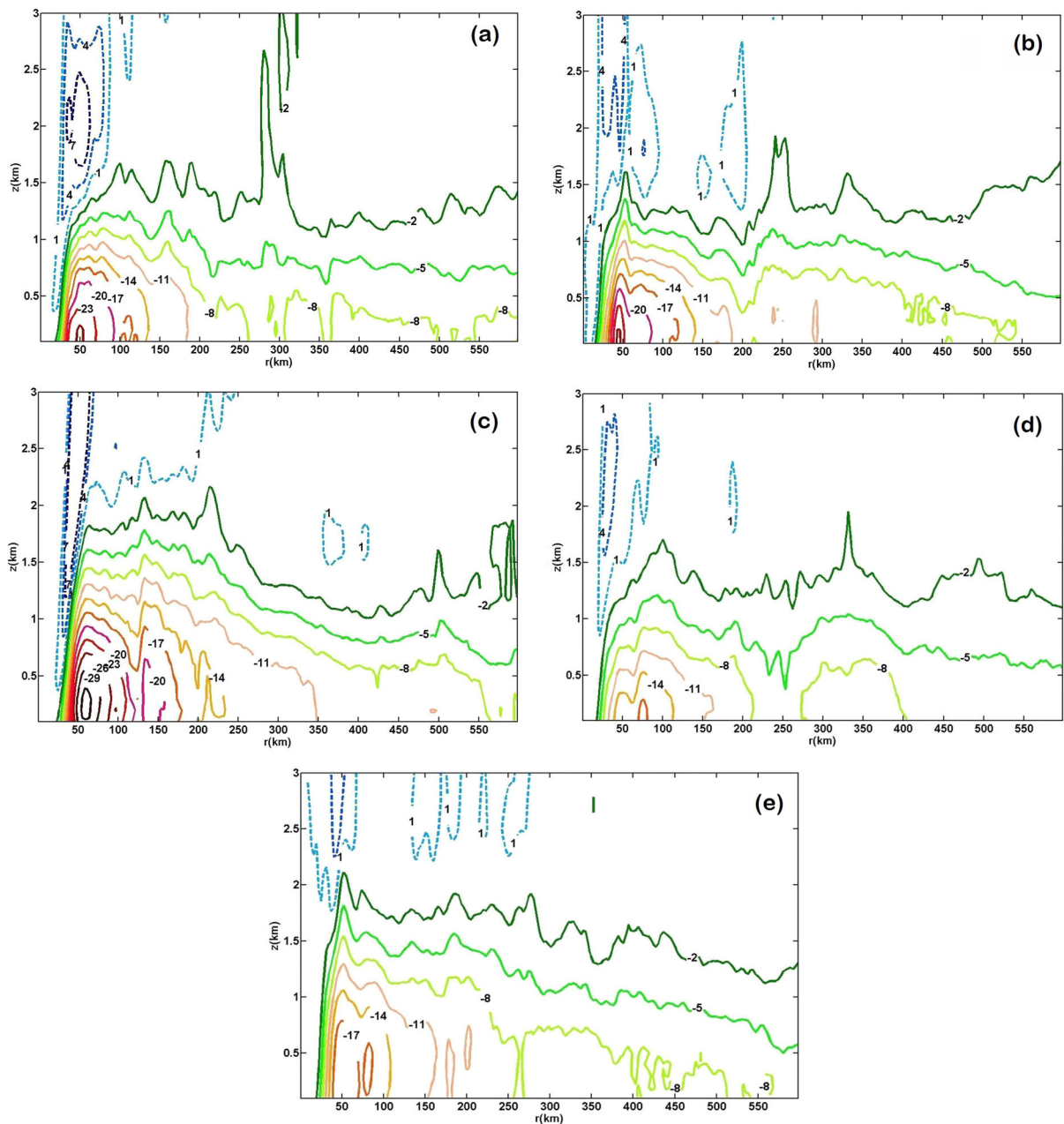
Figure 7
Vertical section of azimuthally averaged radial winds (m/s) for TC Hudhud at 1800 UTC 11 October 2014 from simulations with different PBL physics: **a** YSU, **b** MYJ, **c** QNSE, **d** MYNN, **e** BouLac. Negative values represent the inflow, and positive values represent the outflow

data set (https://disc.gsfc.nasa.gov/datasets/M2T1NX FLX_5.12.4/summary) with a resolution of 0.5° × 0.625° was used for the comparison. Both the latent and sensible heat fluxes steadily increased with time during the development period and rapidly

decreased after the landfall. The differences in the magnitude of the fluxes between simulation and MERRA-2 are obvious due to finer resolution in simulation than the MERRA-2 which is data analyzed over larger areas. The positive values of latent heat
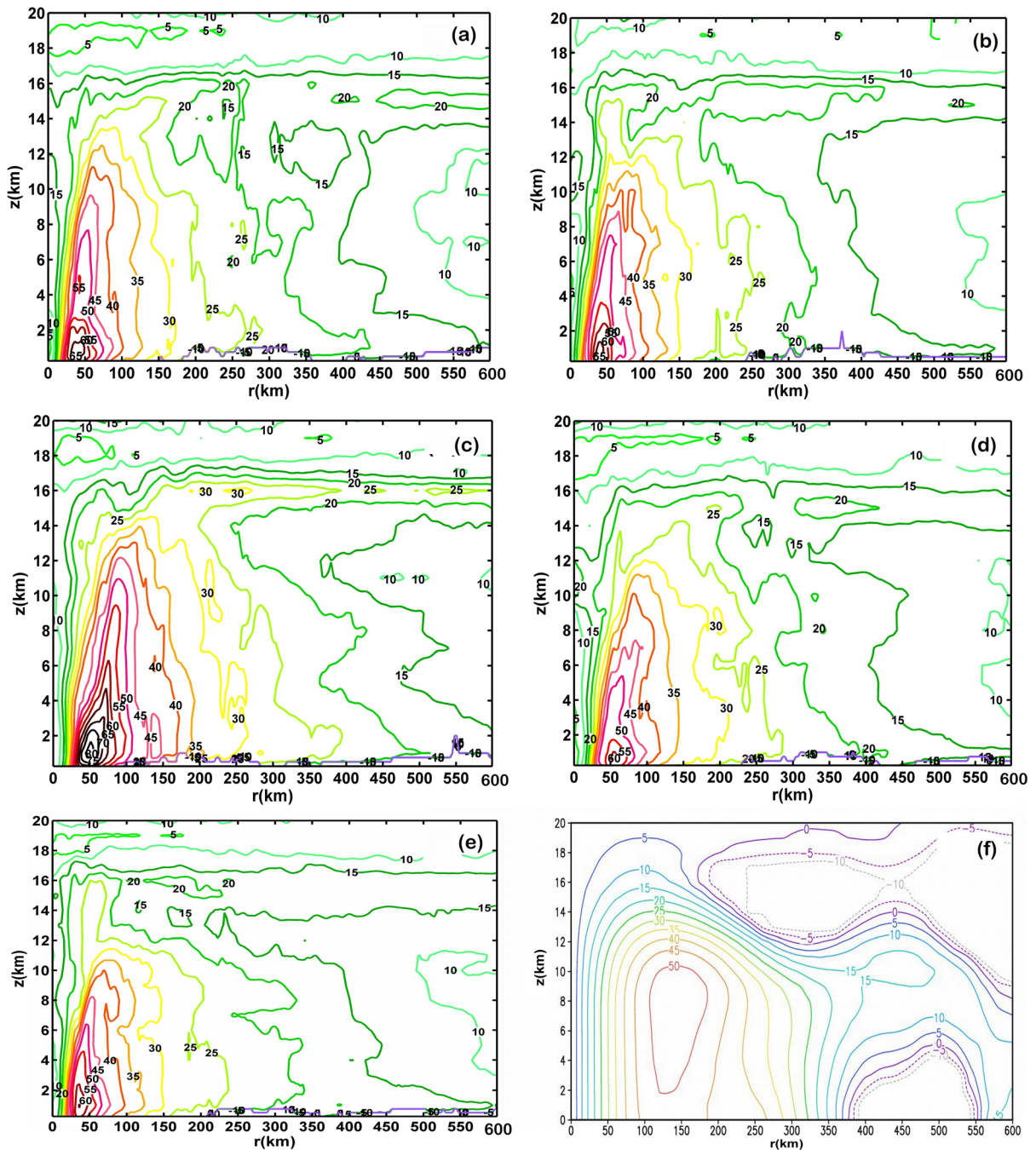
Figure 8
Vertical section of azimuthally averaged tangential winds (m/s) for TC Hudhud at 1800 UTC 11 October 2014 from simulations with different PBL physics: **a** YSU, **b** MYJ, **c** QNSE, **d** MYNN, **e** BouLac, **f** CIRA

flux indicate upward fluxes from the ocean to atmosphere, whereas the negative values indicate the downward transport. From the time series of energy fluxes during the lifecycle of Hudhud (Fig. 9), it is evident that the simulated fluxes are slightly overestimated by YSU and MYNN and grossly
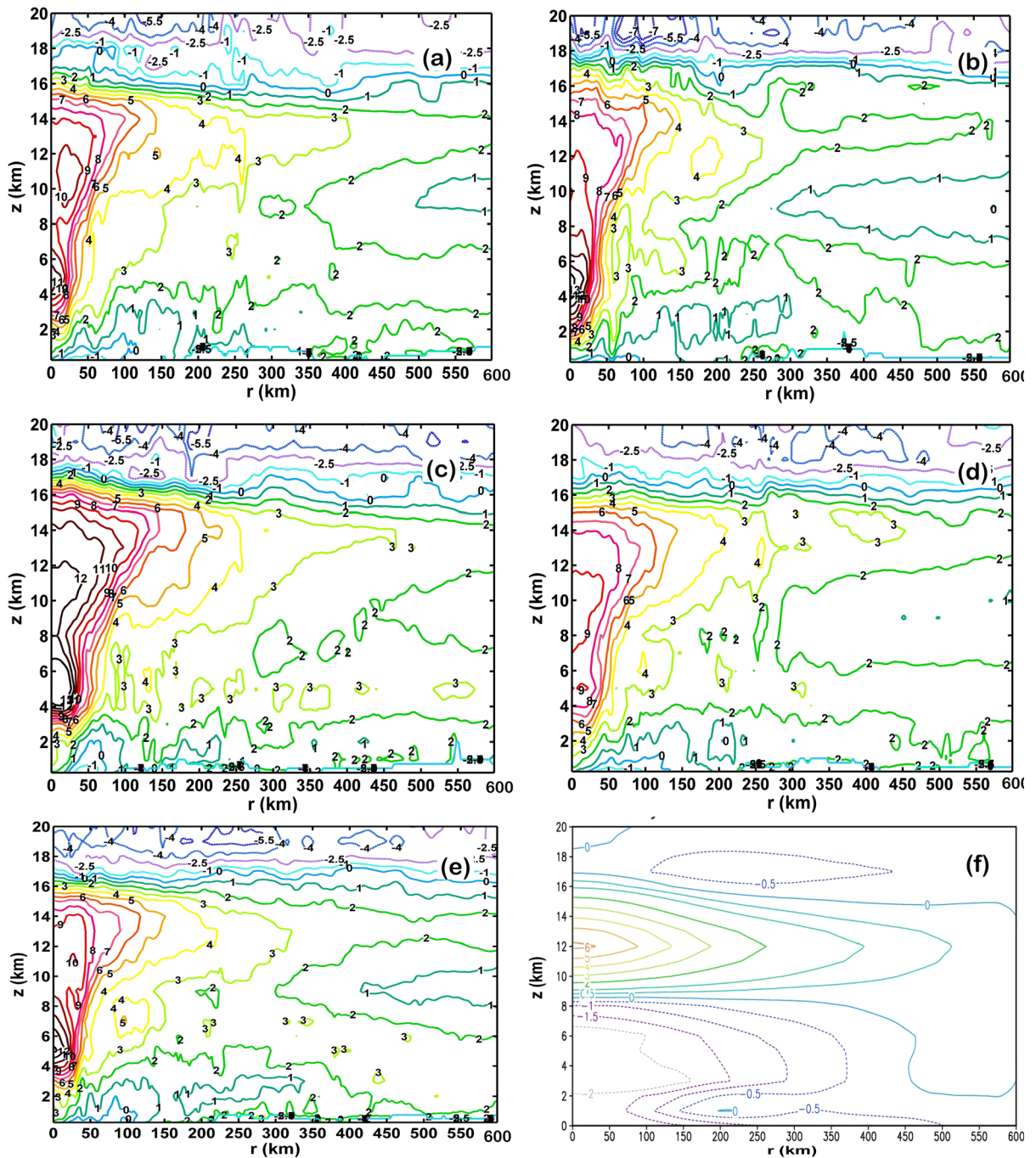
Figure 9
Time variation in energy fluxes averaged over an area of 2° × 2° around the cyclone: **a** latent heat flux, **b** sensible heat flux along the track of TCs along with corresponding values from MERRA-2 reanalysis data

overestimated by QNSE, MYJ and BouLac. The differences are more in latent heat flux which is the main source of energy for the TC (Malkus and Riehl

1960). The same trends are observed in the studies of Avolio et al. (2017) and Hariprasad et al. (2014). The simulated surface energy fluxes in the MYNN and

YSU schemes are nearly similar as the same surface layer scheme (MM5 similarity) is used in these cases. Compared to MYNN, MYJ produced a higher latent and sensible heat flux which is due to the higher surface exchange coefficients for enthalpy in the associated Eta surface layer scheme. The latent heat flux exchange between the ocean to atmosphere increases the available potential energy by releasing the latent heat energy in the clouds, a portion of the released latent heat results in an increase in kinetic energy through an inefficient conversion (Malkus and Riehl 1960; Nolan et al. 2007; Hogsett and Zhang 2009; Ma et al. 2015). The maximum values of heat fluxes are noted during the peak intensity period (12 UTC 11 Oct to 00 UTC 12 Oct) just before the landfall time.

Compared to the latent heat flux, the sensible heat flux is noted to be at least 10 times less. Similar results were reported in Nolan et al. (2009b) for hurricane Isabel. The latent heat flux is crucial to the intensification of the tropical cyclones, whereas the sensible heat flux is more influential for the size of the TC, that is, the TC is shrunk by 20% of its size if we remove the sensible heat flux (Ma et al. 2015).

The intensity of the warm core of TC Hudhud in different simulations is analyzed from the vertical cross section of the azimuthally averaged temperature anomaly (deviation of temperature from its value before the formation of the storm) (Fig. 10). The warming in the upper troposphere is due to

subsidence and adiabatic heating by cloud microphysical processes, whereas the cooling in the lower regions is due to convergence, evaporation, precipitation and downdrafts. These processes affect the intensity of the system through coupling between the thermodynamics and dynamics. The analyzed CIRA data from the Advanced Microwave Sounding Unit (AMSU) azimuthally averaged temperature and height profiles (Demuth et al. 2004) is used for comparison. In the CIRA observation (Fig. 10f), a maximum warming of 6 °C is observed at 12 km, and cooling of -1.5 °C is observed in the lower levels. Because of the coarse nature of CIRA data and the resultant smoothening, the simulation indicates higher warming at the core and more cooling at the lower levels than the CIRA data. The YSU and BouLac schemes produced a warming of 11 °C. The MYJ and QNSE schemes produced the maximum warming (12 °C), and the MYNN produced the minimum warming (9 °C). The simulated warm core strength is in accordance with the latent heat fluxes produced in different simulations (Fig. 9). The strong air–sea interaction associated with the MYJ through higher surface exchange coefficients in the surface layer scheme results in excess transport of moisture and heat in the simulated TC, and excess core warming relative to MYNN. The stronger heat fluxes and stronger wind speeds in the case of the QNSE, MYJ and BouLac schemes suggest a stronger simulated cyclone (Fig. 5b) with a stronger warm core
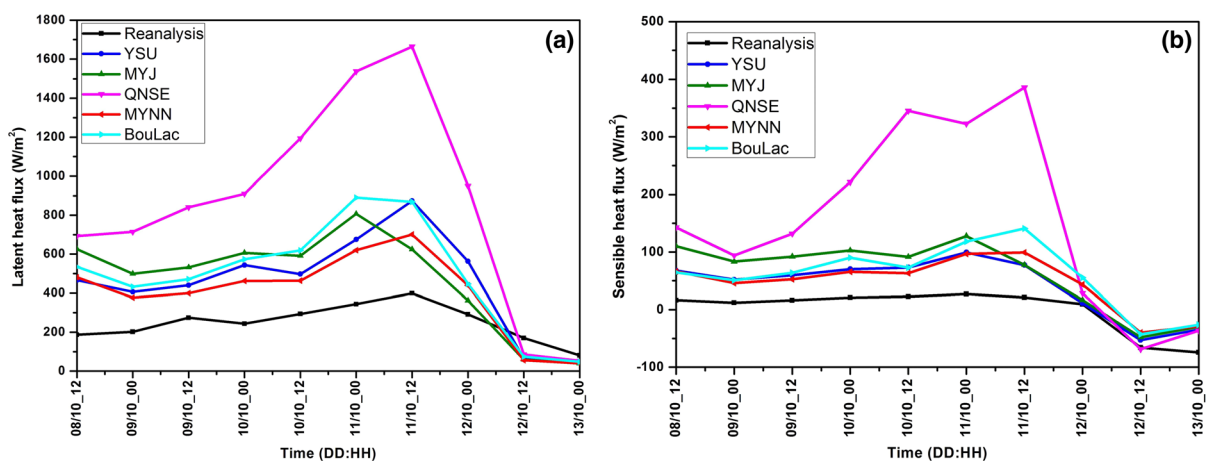

Figure 10
Vertical section of azimuthally averaged temperature anomaly (°C) for TC Hudhud at 1800 UTC 11 October 2014 from simulations with different PBL physics: **a** YSU, **b** MYJ, **c** QNSE, **d** MYNN, **e** BouLac, **f** CIRA

(Fig. 9) according to the wind-induced surface heat exchange (WISHE) theory of TC development (Emanuel, 1986), due to large transport of heat flux from the ocean to the atmosphere by the winds in the inflow layer. Comparison with CIRA data indicates the QNSE and MYJ schemes produced highly intensified cores, while MYNN and BouLac produced a weaker core. Holland (1997) reported that the maximum potential intensity of the TC is highly dependent on the height of the warm core, the relative humidity under the eye wall, and also the short-term changes in the ocean temperature. Together, these features clearly indicate that the upper level warming is better simulated by the YSU, MYJ and MYNN schemes relative to all the other schemes.
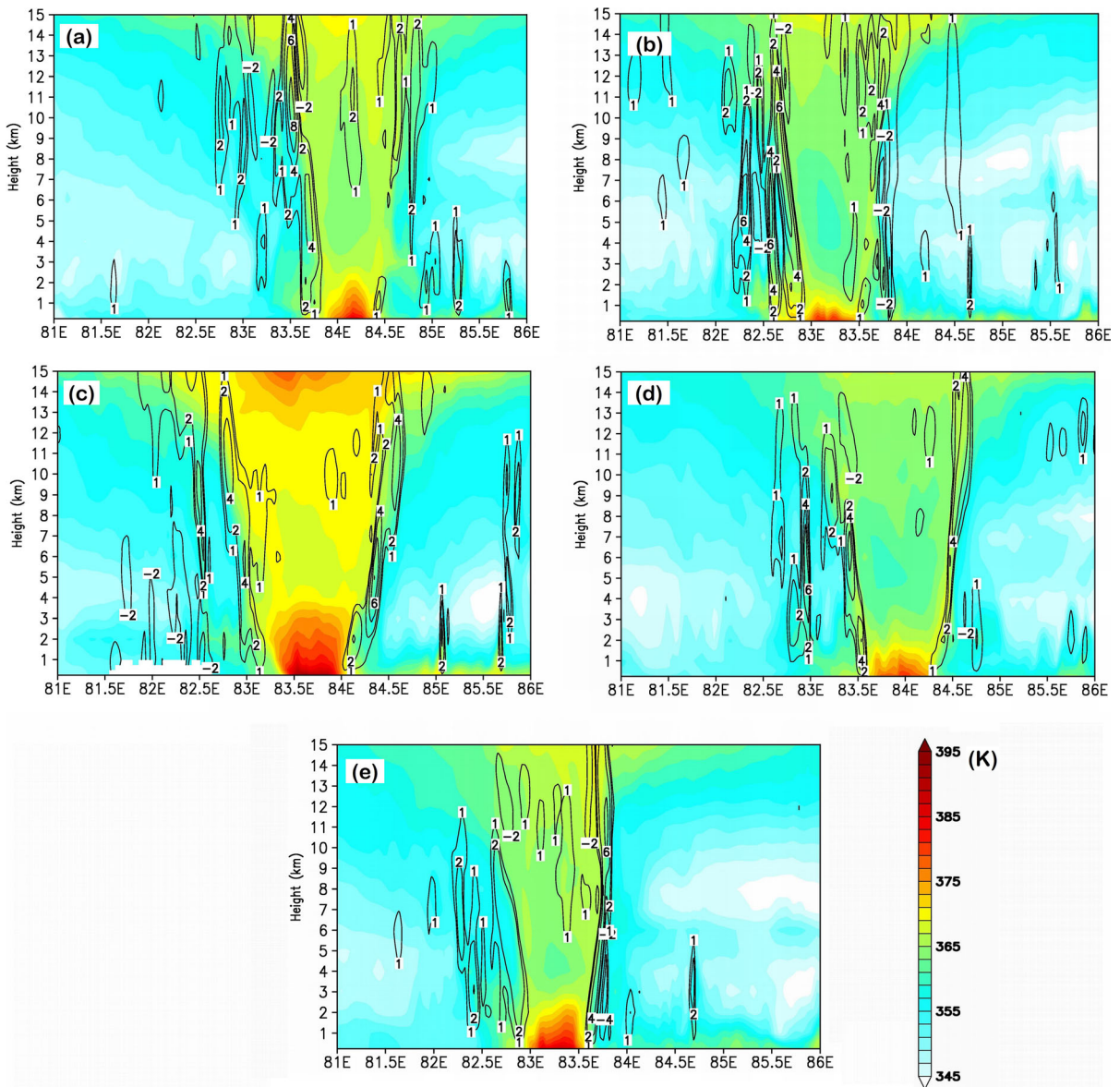

Figure 11

The longitude height cross section of equivalent potential temperature (K) and vertical velocity (m/s) for TC Hudhud at its peak intensity at 1800 UTC 11 October 2014 from simulations with different PBL physics: **a** YSU, **b** MYJ, **c** QNSE, **d** MYNN, **e** BouLac

Figure 11 illustrates the vertical cross-sectional view of equivalent potential temperature (theta-*e*) and the vertical velocity (*w*) distribution of TC Hudhud at 1800 UTC 11 October 2014. The vertical theta-e distribution suggests development of unstable layers in the lower atmosphere (below 5 km), dry regions in the mid-troposphere and stable layers in the upper atmosphere (above 8 km). The high theta-e in the lower regions is due to a stronger convergence of moist air to the center of the TC. Because of continuous transfer of surface fluxes, after some hours, it will become a reservoir of high equivalent potential temperature in the TC (Eastin et al. 2005; Barnes and Fuentes 2010). The QNSE followed by YSU and BouLac produced stronger and larger unstable convective layers in the lower troposphere compared to the MYJ and MYNN schemes. From Fig. 11, it can be observed that the updraft is situated along the eye wall for all the schemes. The YSU, MYJ and QNSE produced stronger updrafts, while MYNN could produce only a moderate value of updrafts along the eye wall. The maximum equivalent potential temperature is distributed within an altitude of 2 km in the simulations with the YSU, MYJ and MYNN schemes, whereas it extended to higher levels in the case of QNSE and BouLac schemes. Among the different simulations, the QNSE shows a relatively wider area of high theta-*e*, indicating large moisture convergence. So the overprediction by this scheme is also quite clear from this analysis. The maximum value of theta-e is predicted by the QNSE scheme (390–395 K), and the MYNN scheme produced the minimum value (378–380 K). The YSU, MYJ and BouLac schemes simulated moderate values of theta-*e* (384–386 K). Even though the variation in the surface exchange coefficients results in more fluxes in the simulation with MYJ compared to the MYNN, the stronger vertical mixing in MYNN results in a relatively deeper unstable layer with a moderate value of theta-e.

Figure 12 shows the average theta-*e*, vertical velocity and divergence over a 2° × 2° area around the center of Hudhud during peak intensification (1800 UTC 11 October 2014). The theta-*e* profile (Fig. 12a) suggests formation of unstable layers below 4.5 km and stable layers above 5 km with a local minimum in theta-e in the mid-troposphere. The

theta-e profiles suggest formation of stronger unstable convective layers in the lower troposphere for QNSE compared to other schemes. The average simulated vertical velocities progressively increased from 2 km onward (Fig. 12b). The QNSE followed by MYJ and BouLac produced higher updraft velocities (40 cm/s for QNSE, 30 cm/s for MYJ, 27 cm/s for BouLac). The YSU produced moderately strong vertical motion (25 cm/s), and MYNN produced weak vertical motion (18 cm/s) in 12–14 km of the upper troposphere. This suggests the convection is strong in the simulations by QNSE, MYJ and BouLac, weak in MYNN and moderate in YSU, and the strength of the warm core varied accordingly in the five simulations. The divergence profile (Fig. 12c) shows that, with the exception of MYNN, all the schemes produce stronger convergence below 2 km and stronger divergence in the upper troposphere (> 12 km). The stronger radial winds in QNSE and MYJ suggest stronger convergence of moist air in the boundary layer (Fig. 12c), stronger vertical motion (Fig. 12b) and thus higher vertical transport of the latent heat flux, producing a stronger warm core in these simulations. The MYNN, due to weaker inflow and convergence, led to relatively weak vertical motions and a weak warm core.

4.3.3 Radar Reflectivity and Rainfall Distribution

Figure 13 shows the spatial distribution of maximum radar reflectivity of TC Hudhud at 0400 UTC 12 October 2014 during the landfall along with corresponding Doppler weather radar (DWR) data at the Visakhapatnam station on the east coast. Maximum radar reflectivity represents areas of deep convection, cloud activity and rainfall. All the simulations show a more intensive cyclone than the actual represented by DWR data. The YSU, MYJ and MYNN schemes produced a well-defined comma cloud band structure. As the QNSE and BouLac schemes simulated faster cyclones, they failed to reproduce the observed cloud band structure at the chosen time due to early landfall and weakening. It is also clear that the YSU and MYNN schemes predicted the actual landfall position in close agreement with DWR observation. It is also clear from the analysis that the well-organized high convective activity and rainfall at the eye wall is not
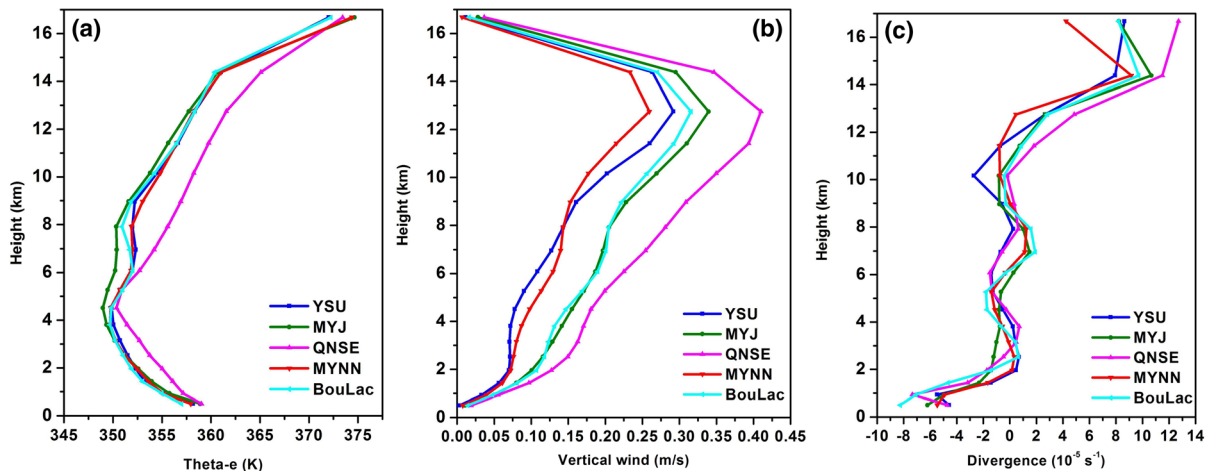
Figure 12

Vertical profiles of **a** theta-e (K), **b** vertical velocity (m/s) and **c** divergence/convergence ($\times 10^{-5}$ s^{-1}) averaged over an area of $2° \times 2°$ from the center of **a** Hudhud at peak intensification from simulations with different PBL physics

present in the case of QNSE and BouLac schemes. Among all the simulations, the YSU and MYNN schemes better produced the region of active convection in close agreement with the DWR observations.

Figure 14 shows the simulated 24-h accumulated rainfall for 00 UTC 12 October–00 UTC 13 October during landfall for TC Hudhud along with corresponding TRMM data (https://mirador.gsfc.nasa.gov/collections/TRMM_3B42_daily__007.shtml). The TRMM data shows symmetric distribution of rainfall, indicating organized convection in a radius of 100 km around Visakhapatnam with maximum rainfall of 175 mm/day. All the simulations predicted higher rainfall, i.e., > 200 mm/day, over land. The MYJ and QNSE simulations produced a relatively high amount of rainfall over wider areas, which could be due to stronger convergence, convection, upward moisture transport facilitated by stronger inflow and larger latent heat flux simulation in these cases. The YSU, MYNN and BouLac schemes show similar rainfall patterns. While none of the simulations could reproduce the observed rainfall distribution, the YSU scheme produced relatively better representation. The rainfall simulated by different PBL schemes varied according to the rate of storm movement, variation in the landfall time and the associated intensity due to moisture availability, etc. Simulations indicate

several smaller areas with relatively high rainfall intensity due to meso-vortices compared to the TRMM data which showed a lesser but uniform rainfall distribution around the center due to coarse resolution (25 km). The cloud band structure simulated by the model with different PBL schemes is influenced by the location of storm (land/sea/along coast) and associated intensity within the 24-h rainfall period considered for comparison. It is seen that the simulated storm in QNSE, BouLac and YSU (to a certain degree) made early landfall. The system in these cases progressed inland to different geographical locations, which results in changes in the moisture and energy transport modulated by the surface characteristics (drag, vegetation, inland water bodies, etc.), finally influencing the organization of clouds and rain band structure differently from the observed pattern.

5. Conclusion

This study examined the impact of PBL physics in the WRF-ARW model on the prediction of intensity and track estimates of tropical cyclones in the Bay of Bengal of the North Indian Ocean. Five conceptually different PBL schemes (YSU, MYJ, QNSE, MYNN and BouLac) were evaluated for their performance in
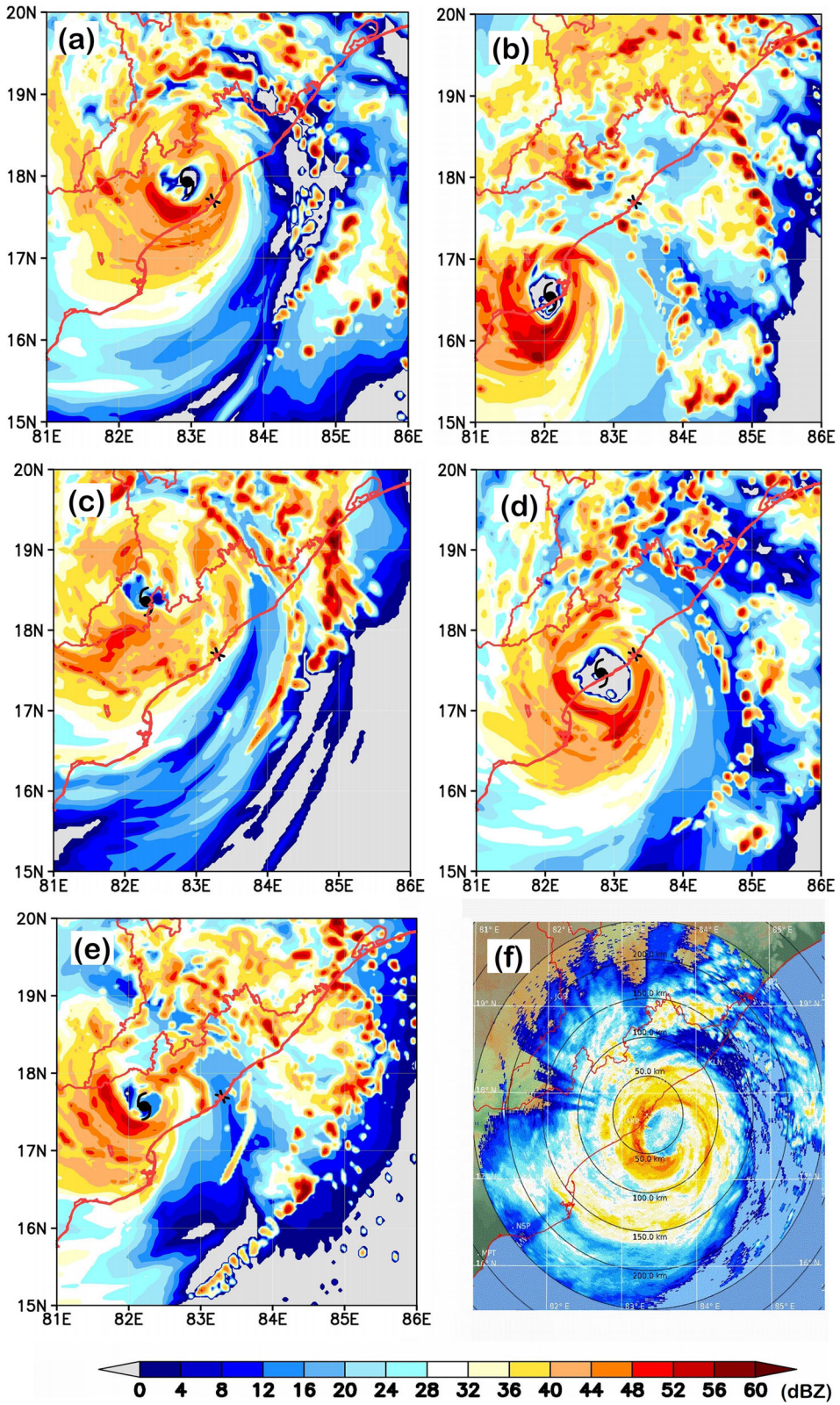
◄Figure 13
Comparison of maximum reflectivity (dBz) for cyclone Hudud from simulations with different PBL physics: **a** YSU, **b** MYJ, **c** QNSE, **d** MYNN, **e** BouLac with **f** DWR observations at Visakhapatnam at 04 UTC 12 October 2014

simulating various features of five very severe tropical cyclones, namely Vardha, Hudhud, Phailin, Lehar and Thane. The results of 25 sensitivity experiments (five cyclones x five PBL schemes) indicated that the non-local YSU scheme produced the best results for both track and intensity predictions. It was found that the simulated mean track errors were lowest with YSU (66, 146, 182, 217 km) and highest with QNSE (63, 163, 198, 242 km) at 24, 48, 72 and 96 h, respectively. The track errors that varied by 5–20% at 24–96-h forecasts indicate the small impact of PBL physics on track prediction.

Considerable differences are found in the CSLP and MSW in the simulations with different PBL physics. The QNSE followed by MYJ and BouLac produced highly intensified storms, and MYNN weakly intensified storms. The YSU scheme produced the lowest CSLP errors (-5.4, -0.8, -2.6, -5.25 hPa), and QNSE produced the highest errors (-5, -8, -11.2, -12 hPa) at 24, 48, 72 and 96 h, respectively. The mean MSW errors for all five cyclones are lowest with YSU (19, 7.6, -0.96, -0.77 m/s) and highest with QNSE (28.5, 16.8, 13.4, 7.0 m/s) at 24, 48, 72 and 96 h, respectively. In general, while MYNN underestimated the winds by $\sim$ 5 to 12% throughout the life cycle, all the other schemes overestimated the winds to different degrees (YSU: -2 to 10%; MYJ: 5 to 22%; BouLac: 8–28%; QNSE: 15–30%). During the period of maximum intensification (48–84 h), the YSU scheme produced the minimum error ($+3$%), followed by MYJ ($+6$%) and MYNN (-10%), while the BouLac and QNSE schemes produced the maximum error of $+22$%. Analysis of various thermodynamical and dynamical parameters clearly showed that the PBL physics impacts the predictions by variation in (1) surface energy fluxes, (2) convergence, (3) inflow/outflow, (4) tangential winds, (5) vertical motion and (6) strength of the warm core and the associated structures. The stronger intensity of TCs simulated by

QNSE, MYJ and BouLac is also associated with stronger convergence, inflow, vertical motions, stronger theta-e and stronger positive vorticity, which represent more convection in these cases.

A detailed analysis for the Hudhud cyclone indicated that the PBL schemes influenced the intensity predictions mainly through a variation in the above parameters. The surface energy fluxes are highly overestimated by QNSE, MYJ and BouLac and simulated in good agreement with MERRA-2 data by YSU and MYNN. The radial inflow and outflow are stronger in the simulations with QNSE and MYJ schemes, moderate with YSU and weaker with MYNN and BouLac schemes. The variation in the radial inflow among different simulations is attributed to the differences in the vertical diffusion and the magnitude of friction/mechanical turbulence in different PBL physics. The surface latent and sensible heat flux plays an important role in the development and maintenance of the tropical cyclone (Byers 1944). The WISHE theory describes a positive feedback between the surface wind speed and transport of energy fluxes to the core, leading to intensification of the storm (Emanuel 1986; Rotunno and Emanuel 1987). The stronger intensification of TCs simulated in the QNSE and MYJ schemes is due to the stronger inflow, spin-up and the stronger wind-induced transport of energy fluxes to the atmosphere giving stronger convection. Though both MYJ and MYNN use the basic Mellor–Yamada PBL formulation, MYJ produced higher intensity than MYNN. The differences in simulations between MYJ and MYNN may be attributed to the differences in the formulation of turbulent length scale and the higher surface exchange coefficient in the Eta surface layer scheme of MYJ. The enhanced upward motions and surface fluxes in the MYJ increases the air interaction and increase the surface energy convergence which in turn strengthen the TC.

Overall, the simulations in this study suggest that YSU produces better intensity and track predictions for the TCs in the Bay of Bengal of the North Indian Ocean. The present study using WRF at a 3-km resolution with YSU and MYJ producing the minimum and maximum track and intensity errors, respectively, confirms the earlier findings by Srinivas et al (2013)
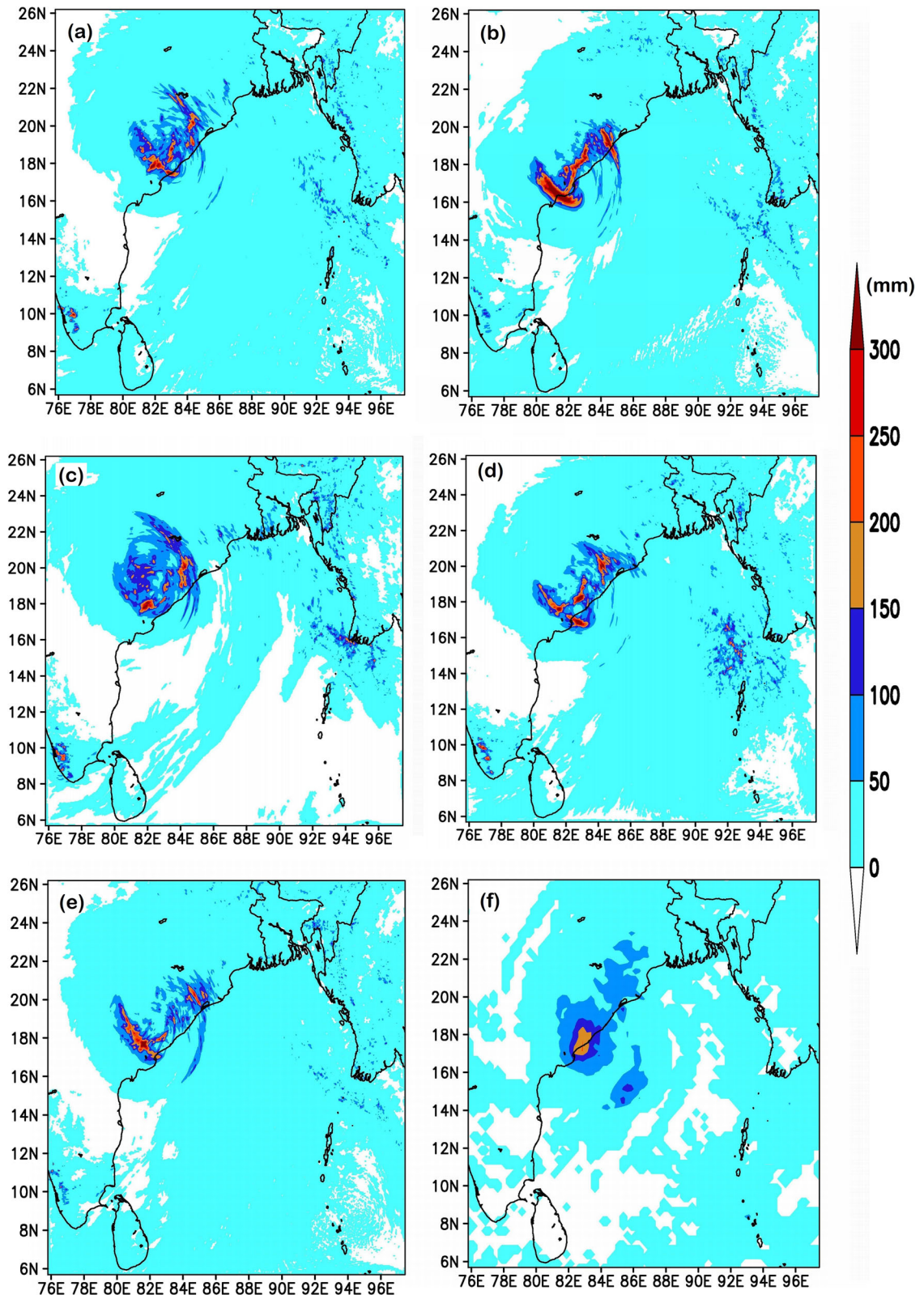
◄Figure 14
Comparison of 24-h accumulated rainfall (mm/day) for Hudhud on the day of landfall (00 UTC 12 October–00 UTC 13 October) from simulations with different PBL physics: **a** YSU, **b** MYJ, **c** QNSE, **d** MYNN, **e** BouLac along with corresponding TRMM observation (**f**)

with 9-km resolution for Sidr and also indicate improved performance for intensity forecasts.

The better performance of YSU over other PBL schemes could be due to better representation of the convective scale eddies through non-local closure and counter-gradient flux terms and explicit inclusion of the entrainment fluxes. The YSU, due to a non-local approach, better represents the effects of strong updraft and downdrafts playing a major role in the development of a TC. The WRF modeling system is widely used for operational weather predictions for monsoons and cyclones and other tropical weather processes over India (Roy Bhowmik 2013). Recent studies with WRF on monsoon rainfall (Hazra and Pattnaik 2020; Rai and Pattnaik 2019) indicate that the PBL physics influences the winds, temperature, humidity and thermodynamics, ultimately impacting the rainfall over different regions, and that the non-local medium-range forecast (MRF) and YSU schemes perform better. The YSU scheme was also shown to produce a more realistic PBL structure during the monsoon (Hariprasad et al. 2014). The better performance of YSU over other complex PBL physics schemes reported by various studies for different weather systems in the Indian region suggests that YSU can be used for both cyclones and monsoon phenomena in operational models.

The present study using high-resolution (3-km) simulations provides greater insight into the PBL physical processes impacting the TC structure, intensity and dynamics compared to the earlier works over the NIO region. The results of this study conducted with more samples of cyclones and with GFS initial and boundary conditions enable us to reduce the uncertainty in operational TC forecasts over the NIO region.

Acknowledgements

Publisher's Note   Springer Nature remains neutral with regard to jurisdictional claims in published maps and institutional affiliations.

References

Avolio, E., Federico, S., Miglietta, M. M., Feudo, T. L., Calidonna, C. R., & Sempreviva, A. M. (2017). Sensitivity analysis of WRF model PBL schemes in simulating boundary-layer variables in southern Italy: an experimental campaign. *Atmospheric Research, 192,* 58–71.

Banks, R. F., Tiana-Alsina, J., Baldasano, J. M., Rocadenbosch, F., Papayannis, A., Solomos, S., et al. (2016). Sensitivity of boundary-layer variables to PBL schemes in the WRF model based on surface meteorological observations, lidar, and radiosondes during the HygrA-CD campaign. *Atmospheric Research, 176,* 185–201.

Barnes, G. M., & Fuentes, P. (2010). Eye excess energy and the rapid intensification of Hurricane Lili (2002). *Monthly Weather Review, 138*(4), 1446–1458.

Bhaskar Rao, D. V., & Hari Prasad, D. (2007). Sensitivity of tropical cyclone intensification to boundary layer and convective processes. *Natural Hazards, 41*(3), 429–445.

Black, P. G., D'Asaro, E. A., Drennan, W. M., French, J. R., Niiler, P. P., Sanford, T. B., et al. (2007). Air–sea exchange in hurricanes: Synthesis of observations from the coupled boundary layer air–sea transfer experiment. *Bulletin of the American Meteorological Society, 88*(3), 357–374.

Bougeault, P., & Lacarrere, P. (1989). Parameterization of orography-induced turbulence in a mesobeta–scale model. *Monthly Weather Review, 117*(8), 1872–1890.

Braun, S. A., & Tao, W. K. (2000). Sensitivity of high-resolution simulations of Hurricane Bob (1991) to planetary boundary layer parameterizations. *Monthly Weather Review, 128*(12), 3941–3961.

Byers, H. R. (1944). Atmospheric turbulence and the wind structure near the surface of the earth. *General meteorology.* New York: McGraw-Hill Book Co., Inc.

Chandrasekar, R., & Balaji, C. (2012). Sensitivity of tropical cyclone Jal simulations to physics parameterizations. *Journal of Earth System Science, 121*(4), 923–946.

Chen, F., & Dudhia, J. (2001). Coupling an advanced land surface–hydrology model with the Penn State–NCAR MM5 modeling system. Part I: Model implementation and sensitivity. *Monthly Weather Review, 129*(4), 569–585.

Davis, C., Wang, W., Chen, S. S., Chen, Y., Corbosiero, K., DeMaria, M., et al. (2008). Prediction of landfalling hurricanes with the advanced hurricane WRF model. *Monthly Weather Review, 136*(6), 1990–2005.

Demuth, J. L., DeMaria, M., Knaff, J. A., & Vonder Haar, T. H. (2004). Evaluation of Advanced Microwave Sounding Unit tropical-cyclone intensity and size estimation algorithms. *Journal of Applied Meteorology, 43*(2), 282–296.

Drennan, W. M., Zhang, J. A., French, J. R., McCormick, C., & Black, P. G. (2007). Turbulent fluxes in the hurricane boundary layer. Part II: Latent heat flux. *Journal of the Atmospheric Sciences, 64*(4), 1103–1115.

Dudhia, J. (1989). Numerical study of convection observed during the winter monsoon experiment using a mesoscale two-dimensional model. *Journal of the Atmospheric Sciences, 46*(20), 3077–3107.

Eastin, M. D., Gray, W. M., & Black, P. G. (2005). Buoyancy of convective vertical motions in the inner core of intense hurricanes. Part II: Case studies. *Monthly Weather Review, 133*(1), 209–227.

Emanuel, K. A. (1986). An air–sea interaction theory for tropical cyclones. Part I: Steady-state maintenance. *Journal of the Atmospheric Sciences, 43*(6), 585–605.

Franklin, J. L., Black, M. L., & Valde, K. (2003). GPS dropwindsonde wind profiles in hurricanes and their operational implications. *Weather and Forecasting, 18*(1), 32–44.

French, J. R., Drennan, W. M., Zhang, J. A., & Black, P. G. (2007). Turbulent fluxes in the hurricane boundary layer. Part I: Momentum flux. *Journal of the Atmospheric Sciences, 64*(4), 1089–1102.

Garratt, J. R. (1994). The atmospheric boundary layer. *Earth-Science Reviews, 37*(1–2), 89–134.

Gopalakrishnan, S. G., Marks, F., Jr., Zhang, X., Bao, J. W., Yeh, K. S., & Atlas, R. (2011). The experimental HWRF system: A study on the influence of horizontal resolution on the structure and intensity changes in tropical cyclones using an idealized framework. *Monthly Weather Review, 139*(6), 1762–1784.

Gopalakrishnan, S. G., Marks, F., Jr., Zhang, J. A., Zhang, X., Bao, J. W., & Tallapragada, V. (2013). A study of the impacts of vertical diffusion on the structure and intensity of the tropical cyclones using the high-resolution HWRF system. *Journal of the Atmospheric Sciences, 70*(2), 524–541.

Gray, W. M. (1968). Global view of the origin of tropical disturbances and storms. *Monthly Weather Review, 96*(10), 669–700.

Greeshma, M., Srinivas, C. V., Hari Prasad, K. B., Baskaran, R., & Venkatraman, B. (2019). Sensitivity of tropical cyclone predictions in the coupled atmosphere–ocean model WRF-3DPWP to surface roughness schemes. *Meteorological Applications, 26*(2), 324–346.

Hariprasad, K. B. R. R., Srinivas, C. V., Singh, A. B., Rao, S. V. B., Baskaran, R., & Venkatraman, B. (2014). Numerical simulation and intercomparison of boundary layer structure with different PBL schemes in WRF using experimental observations at a tropical site. *Atmospheric Research, 145,* 27–44.

Hazra, V., & Pattnaik, S. (2020). Systematic errors in the WRF model planetary boundary layer schemes for two contrasting monsoon seasons over the state of Odisha and its neighborhood region. *Theoretical and Applied Climatology, 139*(3), 1079–1096.

Hill, K. A., & Lackmann, G. M. (2009). Analysis of idealized tropical cyclone simulations using the Weather Research and Forecasting model: Sensitivity to turbulence parameterization and grid spacing. *Monthly Weather Review, 137*(2), 745–765.

Hogsett, W., & Zhang, D. L. (2009). Numerical simulation of hurricane bonnie (1998). Part III: Energetics. *Journal of the Atmospheric Sciences, 66*(9), 2678–2696.

Holland, G. J. (1997). The maximum potential intensity of tropical cyclones. *Journal of the Atmospheric Sciences, 54*(21), 2519–2541.

Holton, J. R. (2004). *Introduction to dynamic meteorology* (4th ed., p. 535). Oxford: Elsevier.

Hong, S. Y., Noh, Y., & Dudhia, J. (2006). A new vertical diffusion package with an explicit treatment of entrainment processes. *Monthly Weather Review, 134*(9), 2318–2341.

Houze, R. A., Chen, S. S., Smull, B. F., Lee, W. C., & Bell, M. M. (2007). Hurricane intensity and eyewall replacement. *Science, 315*(5816), 1235–1239.

Iacono, M. J., Delamere, J. S., Mlawer, E. J., Shephard, M. W., Clough, S. A., & Collins, W. D. (2008). Radiative forcing by long-lived greenhouse gases: Calculations with the AER radiative transfer models. *Journal of Geophysical Research: Atmospheres*, *113*, D13103. https://doi.org/10.1029/2008JD009944.

IMD. (2003). *Cyclone manual*. New Delhi: Published by India Meteorological Department.

Janjić, Z. I. (1994). The step-mountain eta coordinate model: Further developments of the convection, viscous sublayer, and turbulence closure schemes. *Monthly Weather Review, 122*(5), 927–945.

Kain, J. S. (2004). The Kain–Fritsch convective parameterization: an update. *Journal of Applied Meteorology, 43*(1), 170–181.

Kanada, S., Wada, A., Nakano, M., & Kato, T. (2012). Effect of planetary boundary layer schemes on the development of intense tropical cyclones using a cloud-resolving model. *Journal of Geophysical Research: Atmospheres*, *117*, D03107. https://doi.org/10.1029/2011JD016582.

Kepert, J. D. (2006a). Observed boundary layer wind structure and balance in the hurricane core. Part I: Hurricane Georges. *Journal of the Atmospheric Sciences, 63*(9), 2169–2193.

Kepert, J. D. (2006b). Observed boundary layer wind structure and balance in the hurricane core. Part II: Hurricane Mitch. *Journal of the Atmospheric Sciences, 63*(9), 2194–2211.

Kepert, J. D. (2012). Choosing a boundary layer parameterization for tropical cyclone modeling. *Monthly Weather Review, 140*(5), 1427–1445.

Khain, A., Lynn, B., & Shpund, J. (2016). High resolution WRF simulations of Hurricane Irene: Sensitivity to aerosols and choice of microphysical schemes. *Atmospheric Research, 167,* 129–145.

Knaff, J. A., DeMaria, M., Molenar, D. A., Sampson, C. R., & Seybold, M. G. (2011). An automated, objective, multiple-satellite-platform tropical cyclone surface wind analysis. *Journal of Applied Meteorology and Climatology, 50*(10), 2149–2166.

Krishna, K. O., Mohanty, U. C., Routray, A., Kulkarni, M. A., & Mohapatra, M. (2012). Customization of WRF-ARW model with physical parameterization schemes for the simulation of tropical

cyclones over North Indian Ocean. *Natural Hazards, 63*(3), 1337–1359.

Kumari, K. V., Sagar, S. K., Viswanadhapalli, Y., Dasari, H. P., & Rao, S. V. B. (2019). Role of planetary boundary layer processes in the simulation of tropical cyclones over the Bay of Bengal. *Pure and Applied Geophysics, 176*(2), 951–977.

Li, X., & Pu, Z. (2009). Sensitivity of numerical simulations of the early rapid intensification of Hurricane Emily to cumulus parameterization schemes in different model horizontal resolutions. *Journal of the Meteorological Society of Japan Series II, 87*(3), 403–421.

Loh, W. T., Juneng, L., & Tangang, F. T. (2011). Sensitivity of Typhoon Vamei (2001) simulation to planetary boundary layer parameterization using PSU/NCAR MM5. *Pure and Applied Geophysics, 168*(10), 1799–1811.

Ma, Z., Fei, J., Cheng, X., Wang, Y., & Huang, X. (2015). Contributions of surface sensible heat fluxes to tropical cyclone. Part II: The sea spray processes. *Journal of the Atmospheric Sciences, 72*(11), 4218–4236.

Ma, L. M., & Tan, Z. M. (2009). Improving the behavior of the cumulus parameterization for tropical cyclone prediction: Convection trigger. *Atmospheric Research, 92*(2), 190–211.

Malakar, P., Kesarkar, A. P., Bhate, J., & Deshamukhya, A. (2020). Appraisal of data assimilation techniques for dynamical downscaling of the structure and intensity of tropical cyclones. *Earth and Space Science, 7*(2), e2019EA000945.

Malkus, J. S., & Riehl, H. (1960). On the dynamics and energy transformations in steady-state hurricanes. *Tellus, 12*(1), 1–20.

McBride, J. L., & Zehr, R. (1981). Observational analysis of tropical cyclone formation. Part II: Comparison of non-developing versus developing systems. *Journal of the Atmospheric Sciences, 38*(6), 1132–1151.

Mellor, G. L., & Yamada, T. (1974). A hierarchy of turbulence closure models for planetary boundary layers. *Journal of the Atmospheric Sciences, 31*(7), 1791–1806.

Mellor, G. L., & Yamada, T. (1982). Development of a turbulence closure model for geophysical fluid problems. *Reviews of Geophysics, 20*(4), 851–875.

Miglietta, M. M., Mastrangelo, D., & Conte, D. (2015). Influence of physics parameterization schemes on the simulation of a tropical-like cyclone in the Mediterranean Sea. *Atmospheric Research, 153,* 360–375.

Milovac, J., Warrach-Sagi, K., Behrendt, A., Späth, F., Ingwersen, J., & Wulfmeyer, V. (2016). Investigation of PBL schemes combining the WRF model simulations with scanning water vapor differential absorption lidar measurements. *Journal of Geophysical Research: Atmospheres, 121*(2), 624–649.

Miyoshi, T., Komori, T., Yonehara, H., Sakai, R., & Yamaguchi, M. (2010). Impact of resolution degradation of the initial condition on typhoon track forecasts. *Weather and Forecasting, 25*(5), 1568–1573.

Mohan, P. R., Srinivas, C. V., Yesubabu, V., Baskaran, R., & Venkatraman, B. (2019). Tropical cyclone simulations over Bay of Bengal with ARW model: Sensitivity to cloud microphysics schemes. *Atmospheric Research, 230,* 104651.

Mohanty, U. C., Nadimpalli, R., Mohanty, S., & Osuri, K. K. (2019). Recent advancements in prediction of tropical cyclone track over north Indian Ocean basin. *MAUSAM, 70*(1), 57–70.

Montgomery, M. T., Smith, R. K., & Nguyen, S. V. (2010). Sensitivity of tropical-cyclone models to the surface drag coefficient.

Quarterly Journal of the Royal Meteorological Society, 136(653), 1945–1953.

Mukhopadhyay, P., Taraphdar, S., & Goswami, B. N. (2011). Influence of moist processes on track and intensity forecast of cyclones over the north Indian Ocean. *Journal of Geophysics Research, 116,* D05116. https://doi.org/10.1029/2010jd014700.

Nakanishi, M., & Niino, H. (2006). An improved Mellor-Yamada level-3 model: Its numerical stability and application to a regional prediction of advection fog. *Boundary-Layer Meteorology, 119*(2), 397–407.

Nakanishi, M., & Niino, H. (2009). Development of an improved turbulence closure model for the atmospheric boundary layer. *Journal of the Meteorological Society of Japan Series II, 87*(5), 895–912.

Nolan, D. S., Moon, Y., & Stern, D. P. (2007). Tropical cyclone intensification from asymmetric convection: Energetics and efficiency. *Journal of the Atmospheric Sciences, 64*(10), 3377–3405.

Nolan, D. S., Zhang, J. A., & Stern, D. P. (2009a). Evaluation of planetary boundary layer parameterizations in tropical cyclones by comparison of in situ observations and high-resolution simulations of Hurricane Isabel (2003). Part I: Initialization, maximum winds, and the outer-core boundary layer. *Monthly Weather Review, 137*(11), 3651–3674.

Nolan, D. S., Zhang, J. A., & Stern, D. P. (2009b). Evaluation of planetary boundary layer parameterizations in tropical cyclones by comparison of in-situ data and high-resolution simulations of Hurricane Isabel (2003). Part II: inner core boundary layer and eye wall structure. *Monthly Weather Review, 137,* 3675–3698.

Ooyama, K. (1969). Numerical simulation of the life cycle of tropical cyclones. *Journal of the Atmospheric Sciences, 26*(1), 3–40.

Parker, C. L., Lynch, A. H., & Mooney, P. A. (2017). Factors affecting the simulated trajectory and intensification of Tropical Cyclone Yasi (2011). *Atmospheric Research, 194,* 27–42.

Powell, M. D. (1982). The transition of the Hurricane Frederic boundary-layer wind field from the open Gulf of Mexico to landfall. *Monthly Weather Review, 110*(12), 1912–1932.

Raghavan, S., & Sen Sarma, A. K. (2000). Tropical cyclone impacts in India and neighbourhood. *Storms, 1,* 339–356.

Rai, D., & Pattnaik, S. (2018). Sensitivity of tropical cyclone intensity and structure to planetary boundary layer parameterization. *Asia-Pacific Journal of Atmospheric Sciences, 54*(3), 473–488.

Rai, D., & Pattnaik, S. (2019). Evaluation of WRF planetary boundary layer parameterization schemes for simulation of monsoon depressions over India. *Meteorology and Atmospheric Physics, 131*(5), 1529–1548.

Raja Shekhar, S. S., Srinivas, C. V., Rakesh, P. T., Deepu, R., Rao, P. P., Baskaran, R., et al. (2020). Online Nuclear Emergency Response System (ONERS) for consequence assessment and decision support in the early phase of nuclear accidents-Simulations for postulated events and methodology validation. *Progress in Nuclear Energy, 119,* 103177.

Rajeswari, J. R., Srinivas, C. V., Rao, T. N., & Venkatraman, B. (2020). Impact of land surface physics on the simulation of boundary layer characteristics at a tropical coastal station. *Atmospheric Research, 238,* 104888.

Raju, P. V. S., Potty, J., & Mohanty, U. C. (2011). Sensitivity of physical parameterizations on prediction of tropical cyclone

Nargis over the Bay of Bengal using WRF model. *Meteorology and Atmospheric Physics, 113*(3–4), 125.

Raju, P. V. S., Potty, J., & Mohanty, U. C. (2012). Prediction of severe tropical cyclones over the Bay of Bengal during 2007–2010 using high-resolution mesoscale model. *Natural Hazards, 63*(3), 1361–1374.

Rambabu, S., Gayatri, V. D., Ramakrishna, S. S. V. S., Rama, G. V., & AppaRao, B. V. (2013). Sensitivity of movement and intensity of severe cyclone AILA to the physical processes. *Journal of earth system science, 122*(4), 979–999.

Rappaport, E. N., Franklin, J. L., Avila, L. A., Baig, S. R., Beven, J. L., Blake, E. S., et al. (2009). Advances and challenges at the National Hurricane Center. *Weather and Forecasting, 24*(2), 395–419.

Rogers, R., Chen, S., Tenerelli, J., Willoughby, H., et al. (2006). The Intensity Forecasting Experiment: A NOAA multiyear field program for improving tropical cyclone intensity forecasts. *Bulletin of the American Meteorological Society, 87*(11), 1523–1537.

Rotunno, R., & Emanuel, K. A. (1987). An air–sea interaction theory for tropical cyclones. Part II: Evolutionary study using a nonhydrostatic axisymmetric numerical model. *Journal of the Atmospheric Sciences, 44*(3), 542–561.

Roy Bhowmik, S. K. (2013). Operational Numerical Weather Prediction (NWP) System of IMD. Retrieved from: http://www.imd.gov.in/doc/nwpsystem.pdf. Accessed 13 Mar 2020.

Saikumar, P. J., & Ramashri, T. (2017). Impact of physics parameterization schemes in the simulation of Laila cyclone using the advanced mesoscale weather research and forecasting model. *International Journal of Applied Engineering Research, 12*(22), 12645–12651.

Singh, K. S., & Bhaskaran, P. K. (2017). Impact of PBL and convection parameterization schemes for prediction of severe land-falling Bay of Bengal cyclones using WRF-ARW model. *Journal of Atmospheric and Solar-Terrestrial Physics, 165*, 10–24.

Skamarock, W. C., Klemp, J. B., Dudhia, J., Gill, D. O., Barker, D. M., & Duda, M. (2008). *A Description of the Advanced Research WRF Version 3 (technical note NCAR/TN-475 + STR)*. Boulder, CO: National Center for Atmospheric Research.

Smith, R. K., & Thomsen, G. L. (2010). Dependence of tropical-cyclone intensification on the boundary-layer representation in a numerical model. *Quarterly Journal of the Royal Meteorological Society, 136*(652), 1671–1685.

Srinivas, C. V., Bhaskar Rao, D. V., Yesubabu, V., Baskaran, R., & Venkatraman, B. (2013). Tropical cyclone predictions over the Bay of Bengal using the high-resolution Advanced Research Weather Research and Forecasting (ARW) model. *Quarterly Journal of the Royal Meteorological Society, 139*(676), 1810–1825.

Srinivas, C. V., Venkatesan, R., Rao, D. B., & Prasad, D. H. (2007). Numerical simulation of Andhra severe cyclone (2003): Model sensitivity to the boundary layer and convection parameterization. *Atmospheric and oceanic* (pp. 1465–1487). Basel: Birkhäuser.

Srinivas, C. V., Yesubabu, V., Prasad, D. H., Prasad, K. H., Greeshma, M. M., Baskaran, R., et al. (2018). Simulation of an extreme heavy rainfall event over Chennai, India using WRF: Sensitivity to grid resolution and boundary layer physics. *Atmospheric Research, 210*, 66–82.

Stensrud, D. J. (2007). *Parameterization schemes: Keys to understanding numerical weather prediction models, 459*. Cambridge, UK: Cambridge University Press.

Stull, R. B. (1988). *An introduction to boundary layer meteorology* (p. 680). Dordrecht, Holland: Kluwer.

Sukoriansky, S., Galperin, B., & Perov, V. (2005). Application of a new spectral theory of stably stratified turbulence to the atmospheric boundary layer over sea ice. *Boundary-Layer Meteorology, 117*(2), 231–257.

Thompson, G., Field, P. R., Rasmussen, R. M., & Hall, W. D. (2008). Explicit forecasts of winter precipitation using an improved bulk microphysics scheme Part II: Implementation of a new snow parameterization. *Monthly Weather Review, 136*(12), 5095–5115.

Wada, A., & Usui, N. (2010). Impacts of oceanic preexisting conditions on predictions of Typhoon Hai-Tang in 2005. *Advances in Meteorology, 2010*, 756071. https://doi.org/10.1155/2010/756071.

Zhang, D., & Anthes, R. A. (1982). A high-resolution model of the planetary boundary layer—sensitivity tests and comparisons with SESAME-79 data. *Journal of Applied Meteorology*, *21*(11), 1594–1609.

Zhang, J. A., Black, P. G., French, J. R., & Drennan, W. M., (2008). First direct measurements of enthalpy flux in the hurricane boundary layer: The CBLAST results. *Geophysical Research Letters*, *35*, L14813. https://doi.org/10.1029/2008GL034374.